Supporting Information for:

A Mitochondria-Targeted Cryptocyanine-Based Photothermogenic Photosensitizer

Hyo Sung Jung,[†,§] Jae-Hong Lee,[‡] Kyutae Kim,[‡] Seyoung Koo,[†] Peter Verwilst,[†] Jonathan L. Sessler,*[,§] Chulhun Kang,*[,‡] and Jong Seung Kim*[,†]

[†]Department of Chemistry, Korea University, Seoul 02841, Korea
[‡]The Graduate School of East-West Medical Science, Kyung Hee University, Yongin 17104, Korea
[§]Department of Chemistry, The University of Texas at Austin, Austin, Texas 78712-1224, United States

*E-mail: sessler@cm.utexas.edu; kangch@khu.ac.kr; jongskim@korea.ac.kr

● Synthesis of photo-thermal cryptocyanines

Compound **4** was synthesized according to reported procedures.[1]

Compound **3**: A mixture of 4-methylquinoline (1.59 mL, 12.0 mmol) and 4-(bromomethyl)benzoic acid (2.15 g, 10.0 mmol) in anhydrous acetonitrile was stirred at 110 °C for 6 h under a nitrogen atmosphere. The solvent was evaporated off and the residue was dissolved in methanol (3 mL) at which point diethyl ether (30 mL) was added slowly. The precipitate was collected by filtration, washed with diethyl ether, and dried under vacuum to yield compound **3** as a white solid (3.1 g, 72%): ^{1}H NMR (400 MHz, MeOH-d_4): δ 9.43 (d, J = 6.06 Hz, 1H), 8.60 (dd, J = 8.45 Hz, 1H), 8.38 (d, J = 8.91 Hz, 1H), 8.15 (t, J = 8.66 Hz, 1H), 8.09 (dd, J = 6.06 Hz, 1H), 8.05-8.00 (m, 3H), 7.40 (d, J = 8.72 Hz, 2H), 6.39 (s, 2H), 3.12 (s, 3H). ^{13}C NMR (100 MHz, DMSO-d_6): 166.9, 160.0, 149.6, 139.1, 137.0, 135.5, 131.0, 130.1, 129.9, 129.4, 127.5, 127.4, 123.2, 119.8, 59.2, 20.1. ESI-MS calc. for $C_{18}H_{16}NO_2$ $[M\text{-}Br]^+$ 278.12, found 278.15.

Compound **2**: A mixture of **3** (1.79 g, 5.00 mmol) and *N*,*N*′-diphenylformamidine (1.96 g, 10.0 mmol) in acetic anhydride (10 mL) was stirred at 150 °C for 1 h. After the mixture was cooled to room temperature, diethyl ether (100 mL) was added slowly. The precipitate was collected by filtration, washed with diethyl ether, and dried under vacuum to yield compound **2** as a brown solid (2.20 g, 87%): ^{1}H NMR (400 MHz, DMSO-d_6): δ 9.39 (d, J = 6.61 Hz, 1H), 8.97 (d, J = 13.83 Hz, 1H), 8.49 (d, J = 6.75 Hz, 1H), 8.20 (d, J = 8.87 Hz, 1H), 8.04 (t, J = 9.10 Hz, 1H), 7.96-7.88 (m, 4H), 7.81 (t, J = 8.67 Hz, 1H), 7.72-7.64 (m, 2H), 7.53 (d, J = 7.40 Hz, 2H), 7.37 (d, J = 8.67 Hz, 2H), 6.29 (s, 2H), 6.07 (d, J = 13.98 Hz, 1H), 2.10 (s, 3H). ^{13}C NMR (100 MHz, DMSO-d_6): 170.0, 166.8, 154.1, 147.9, 142.0, 139.4, 137.9, 137.6, 135.1, 130.6, 130.0, 129.8, 129.7, 129.5, 129.2, 128.6, 127.6, 127.2, 127.0, 126.7, 126.0, 125.4, 119.5, 115.2, 102.9, 58.5, 23.4. ESI-MS calc. for $C_{27}H_{23}N_2O_3$ $[M\text{-}Br]^+$ 423.17, found 423.2.

Compound **1**: A mixture of **2** (0.422 g, 1.0 mmol), **3** (0.362 g, 1.00 mmol) and triethylamine (1.40 mL, 10.0 mmol) in dichloromethane (20 mL) was stirred at 25 °C for 24 h. The solvent was evaporated off and the residue was dissolved in methanol (1 mL) after which acetone (250 mL) was added slowly. The precipitate was collected by filtration, washed with acetone, and dried under vacuum to yield compound **1** as a blue solid (0.304 g, 46%): ^{1}H NMR (500 MHz, DMSO-d_6): δ 8.83 (t, J = 13.44 Hz, 1H), 8.40 (m, 4H), 7.95-7.91 (m, 6H), 7.73-7.67 (m, 4H), 7.57 (t, J = 7.44 Hz, 2H), 7.38 (d, J = 8.40 Hz, 4H), 7.21 (d, J = 13.08 Hz, 2H), 5.81 (s, 4H). ^{13}C NMR (125

MHz, DMSO-d_6): 166.9, 148.9, 143.5, 141.6, 141.0, 138.2, 132.8, 130.4, 130.0, 129.5, 127.6, 126.7, 126.1, 125.0, 124.4, 117.8, 111.5, 109.0, 55.9. ESI-MS calc. for $C_{37}H_{29}N_2O_4$ [M +Na-Br-2H]$^-$ 586.21, found 586.40.

CCy: A mixture of **1** (0.410 g, 0.640 mmol), *N*,*N*′-diisopropylethylamine (111 μL, 0.640 mmol) and HATU (0.240 g, 0.640 mmol) in DMF (5 mL) was stirred at 25 °C for 30 min. Propylamine (130 μL, 1.58 mmol) and triethylamine (221 μL, 1.58 mmol) were added to the reaction mixture, and stirred at 25 °C for 24 h. After removal of the DMF solvent under vacuum, the crude product was purified by column chromatography over silica gel using CH_2Cl_2/MeOH (v/v, 95:5) as the eluent. After removing of the volatiles, this gave **CCy** as a blue solid (0.153 g, 32%): ^{1}H NMR (500 MHz, DMSO-d_6): δ 8.82 (t, J = 13.44 Hz, 1H), 8.44 (t, J = 6.48 Hz, 2H), 8.39 (d, J = 7.69 Hz, 4H), 7.91 (d, J = 7.54 Hz, 2H), 7.82 (d, J = 8.40 Hz, 4H), 7.75-7.68 (m, 4H), 7.56 (t, J = 8.45 Hz, 2H), 7.36 (d, J = 8.40 Hz, 4H), 7.20 (d, J = 13.03 Hz, 2H), 5.77 (s, 4H), 3.19 (q, J = 6.50 Hz, 4H), 1.50 (m, 4H), 0.86 (t, J = 7.15 Hz, 6H). ^{13}C NMR (125 MHz, DMSO-d_6): 165.7, 148.9, 143.4, 141.6, 139.0, 138.1, 134.5, 132.7, 127.8, 126.4, 126.1, 125.0, 124.4, 117.9, 111.4, 108.9, 55.9, 41.0, 22.4, 11.4. ESI-MS calc. for $C_{43}H_{43}BrN_4O_2$ [M-Br]$^+$ 647.34, found 647.35.

Mito-CCy: A mixture of **1** (0.410 g, 0.640 mmol), *N*,*N*-diisopropylethylamine (111 μL, 0.640 mmol) and HATU (0.242 g, 0.640 mmol) in DMF (5 mL) was stirred at 25 °C for 30 min. $(PPh_3^+(CH_2)_2NH_2)Br^-$ (0.610 g, 1.58 mmol) and triethylamine (220 μL, 1.58 mmol) were added to a reaction mixture, and stirred at 25 °C for 24 h. After removal of DMF under vacuum, the crude product was purified by column chromatography over silica gel using CH_2Cl_2/MeOH (*v*/*v*, 95:5) as the eluent. After removal of the volatiles, this gave **Mito-CCy** as a blue solid (0.304 g, 34%): ^{1}H NMR (500 MHz, MeOH-d_4/DMSO-d_6): δ 8.81 (t, J = 13.44 Hz, 1H), 8.50 (d, J = 7.82 Hz, 2H), 8.25 (m, 2H), 7.96-7.88 (m, 20H), 7.81-7.75 (m, 20H), 7.71 (d, J = 8.54 Hz, 2H), 7.60 (t, J = 8.26 Hz, 2H), 7.41 (d, J = 7.99 Hz, 4H), 7.25 (d, J = 12.67 Hz, 2H), 5.77 (s, 4H), 3.89-3.82 (m, 4H), 3.81-3.76 (m, 4H). ^{13}C NMR (125 MHz, MeOH-d_4/DMSO-d_6): 168.6, 150.8, 144.5, 142.6, 141.1, 139.7, 136.5, 136.4, 135.0, 134.9, 134.6, 134.0, 131.6, 131.5, 129.3, 127.8, 127.4, 126.5, 126.1, 119.9, 119.2, 118.9, 112.9, 110.1, 57.7, 34.9, 23.1. ESI-MS calc. for $C_{77}H_{67}Br_3N_4O_2P_2$ [M-3Br-3H]$^+$ 1138.47, found 1138.3.

Calculation of the fluorescence quantum yield

Fluorescence quantum yields (Φ_f) were measured by comparing the fluorescence intensity of the sample with that of a fluorescence reference according to the following equation:

$$\Phi_f(PS) = \Phi_f(ref)\left(\frac{A_{PS}}{A_{ref}}\right)\left(\frac{{n_{PS}}^2}{{n_{ref}}^2}\right) \quad \text{----- equation (S1)}$$

where, A_{ps} and A_{ref} are the integrated area under the corrected fluorescence spectra for the sample and reference, n_{ps} and n_{ref} are the refractive indexes of the sample and reference, respectively. Zinc phthalocyanine in toluene containing 1.0% pyridine, which has a known quantum yield of 0.30,[2] was used as the reference.

Calculation of the photothermal conversion efficiency

The photothermal conversion efficiencies (η) were measured according to a previously described method:[3]

$$\eta = \frac{hs(T_{Max} - T_{Surr}) - Q_{Dis}}{I(1-10^{-A_{730}})} \quad \text{----- equation (S2)}$$

h is the heat transfer coefficient, s is the surface area of the container, and the value of hs is determined from the equation (3). Q_{Dis} represents heat dissipated from the laser mediated by the solvent and container. I is the laser power and A is the absorbance at 730 nm.

$$hs = \frac{mC}{\tau_S} \quad \text{----- equation (S3)}$$

m is the mass of the solution containing the photoactive material, C is the specific heat capacity of the solution, and τ_S is the associated time constant, which can be determined from equation (S4).

$$t = -\tau_S \ln(\theta) \quad \text{----- equation (S4)}$$

θ is a dimensionless parameter, known as the driving force temperature, as calculated using equation (S5).

$$\theta = \frac{T - T_{Surr}}{T_{Max} - T_{Surr}} \quad \text{----- equation (S5)}$$

T_{max} and T_{Surr} are the maximum steady state temperature and the environmental temperature, respectively.

● Calculation of singlet oxygen quantum yields

Singlet oxygen quantum yields (Φ_Δ) were calculated using a previously described method.[4] The relative quantum yields were calculated with reference to Methylene Blue (MB) in DMSO for which the quantum yield is 0.52.[5] Air saturated DMSO was obtained by bubbling with air for 15 minutes. The absorbance of 1,3-diphenylisobenzofuran (DPBF) or 9,10-anthracenediyl-bis(methylene)dimalonic acid (ABDA) was adjusted by modifying the concentration such that it was around 1.0 in air saturated solvent. Samples were added to a cuvette and the absorbance of the putative photosensitizer (PS) in question was then adjusted to around 0.1. After measurements were taken in the dark, the cuvette was exposed to monochromatic light at the peak absorption wavelength for 3 or 5 minutes. The absorbance was measured several times after each irradiation. The recorded data are shown in Figs. S7-9. The absorbance maxima of DPBF at 408 nm was then plotted versus the time and the slope determined for each PS. Singlet oxygen quantum yields were calculated according to the equation:

$$\Phi_\Delta(PS) = \Phi_\Delta(ref) \times \left(\frac{m_{PS}}{m_{ref}}\right) \times \left(\frac{F_{ref}}{F_{PS}}\right) \times \left(\frac{PF_{ref}}{PF_{PS}}\right) \qquad \text{----- equation (S6)}$$

where m is the slope of a plot of the change in absorption of DPBF at 408 nm at the irradiation time in question as recorded in the presence of the PS, F is the absorption correction factor, which can be determined by $F = 1 - 10^{-OD}$ (OD at the irradiation wavelength), and PF is an absorbed photonic flux (μEinstein dm^{-3} s^{-1}).

● Cell Culture and Confocal Microscopy Studies

HeLa cells (KCLB, Seoul, Korea) were cultured in DMEM (WelGene Inc, Seoul, Korea) with 10% FBS (WelGene), and penicillin (100 units/ml). All cells were maintained in a humidified atmosphere of 5/95 (*v*/*v*) of CO_2/air at 37 °C. The cells were treated and incubated with **Mito-CCy** at 37 °C under 5% CO_2 during the time mentioned in the text. For the confocal microscopic samples, the cells were passed and plated on glass bottomed dishes (MatTek). The cells were washed three times with phosphate buffered saline (PBS; Gibco) and then imaged after further incubation in colorless serum-free media for 15 min. fluorescence microscopy images of labeled cells were obtained with spectral confocal microscopes (Leica TCS SP2 and Zeiss model LSM 510) with ×10, × 40 dry and ×100 oil objectives, numerical aperture (NA) = 0.30, 0.75 and 1.30.

Two-photon fluorescence microscopy images were obtained with a DM IRE2 Microscope (Leica) by exciting the probes with a mode-locked titanium-sapphire laser source (Coherent Chameleon, 90 MHz, 200 fs) set at wavelength 740 nm and an output power of 1260 mW; this corresponds to approximately 5 mW average power in the focal plane. To obtain images over the 550-650 nm spectral range, (Leica TCS SP2) and long path (>650 nm, Zeiss model LSM 510) internal PMTs were used to collect the signals in 8 bit unsigned 512 × 512 and 1024 × 1024 pixel format at scan speeds of 800 and 400 Hz, respectively. Tracking dyes for co-localization experiments were bought from Invitrogen. Other information is available in the figure captions

- **Cytotoxicity Assays**

HeLa cells (2.0×10^5 per dish) were seeded on 35 mm confocal dishes and allowed to stabilize for 48 h. The cells were then treated with different concentration **Mito-CCy** (0, 5, 10, 15, and 20 μM) in 1 mL culture medium. After 4 h incubation, the cells were irradiated with a 730 nm pulsed laser (2.3 W/cm^2) for 10 min to induce photothermal cytotoxicity. The mode of cell death was examined by using a Hoechst 33342 (0.2 μM) and propidium iodide (0.2 μM) staining kit according to manufacturer's instructions (Invitrogen). The results in HeLa cells were monitored under a confocal fluorescence microscope.

- **Detection of mitochondrial ROS formation**

HeLa cells (2.0×10^5 per dish) were seeded on 35 mm confocal dishes and allowed to stabilize for 48 h. The cells were then incubated with medium containing **Mito-CCy** (10 μM) for 3.5 h and washed three times with PBS. Antimycin A (0.5 μM), rotenone (0.5 μM), or Antimycin A (0.5 μM) with rotenone (0.5 μM) in 1 mL culture medium was then added. After 30 min incubation, the cells were irradiated with a 730 nm pulsed laser (2.3 W/cm^2) for 10 min. The amount of ROS generated was determined using the MitoSOX (1 μM) staining kit according to the manufacturer's instructions (Invitrogen). The results in HeLa cells were monitored using a confocal fluorescence microscope. For SOD-related experiment, HeLa cells (2.0×10^5 per dish) were also seeded using a similar procedure. The cells were then incubated with medium containing 2-methoxyestradiol (2 μM) for 1 h and washed three times with PBS. **Mito-CCy** (10 μM) in 1 mL of culture medium was

then added and the cells incubated for 4 h. The cells were then irradiated with a 730 nm pulsed laser (2.3 W/cm^2) for 10 min. The amount of ROS generated was determined using the MitoSOX (1 μM) staining kit according to the manufacturer's instructions (Invitrogen).

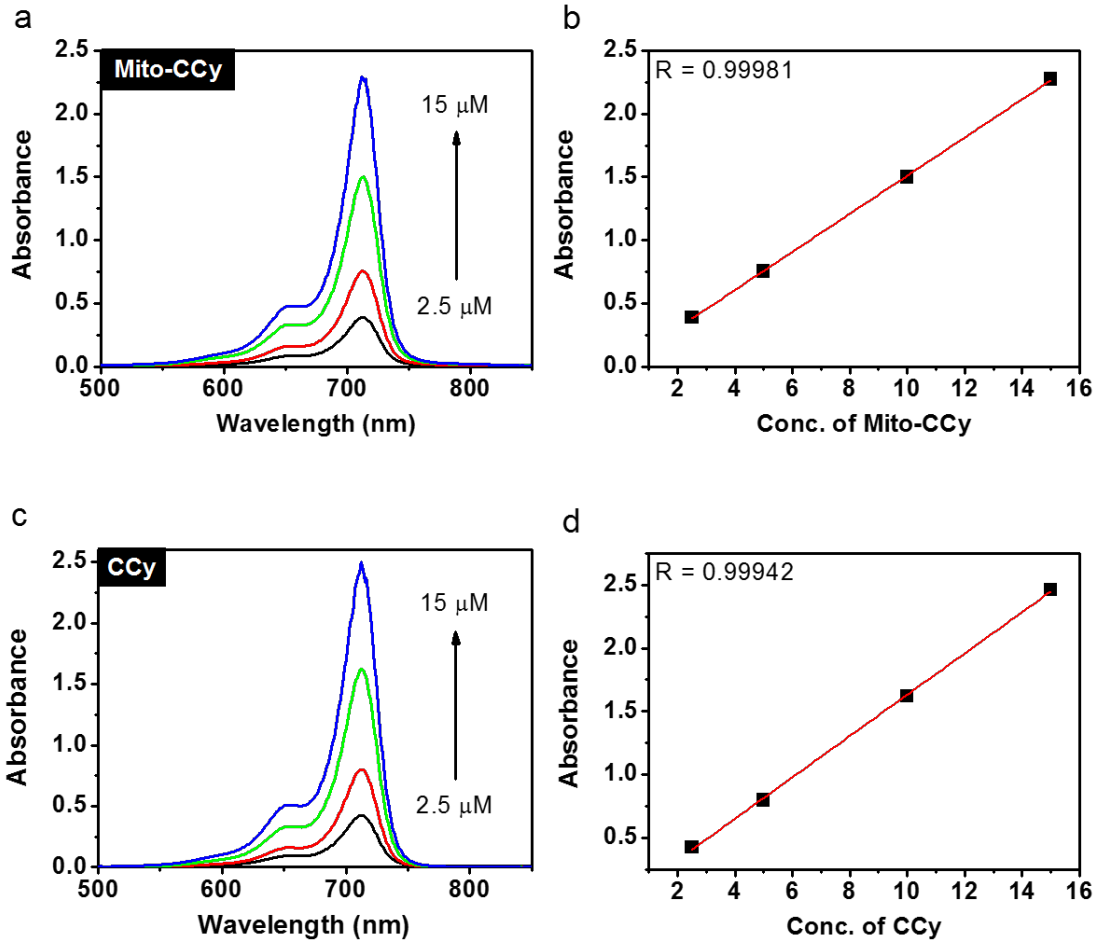

Figure S1. Absorption spectra of (a) **Mito-CCy** and (c) **CCy** at various concentrations (i.e., 2.5, 5.0, 10 and 15 μM) in DMSO solution. Linear relationship seen in plots of the absorbance at 713 nm vs (b) **Mito-CCy** or (d) **CCy** concentration.

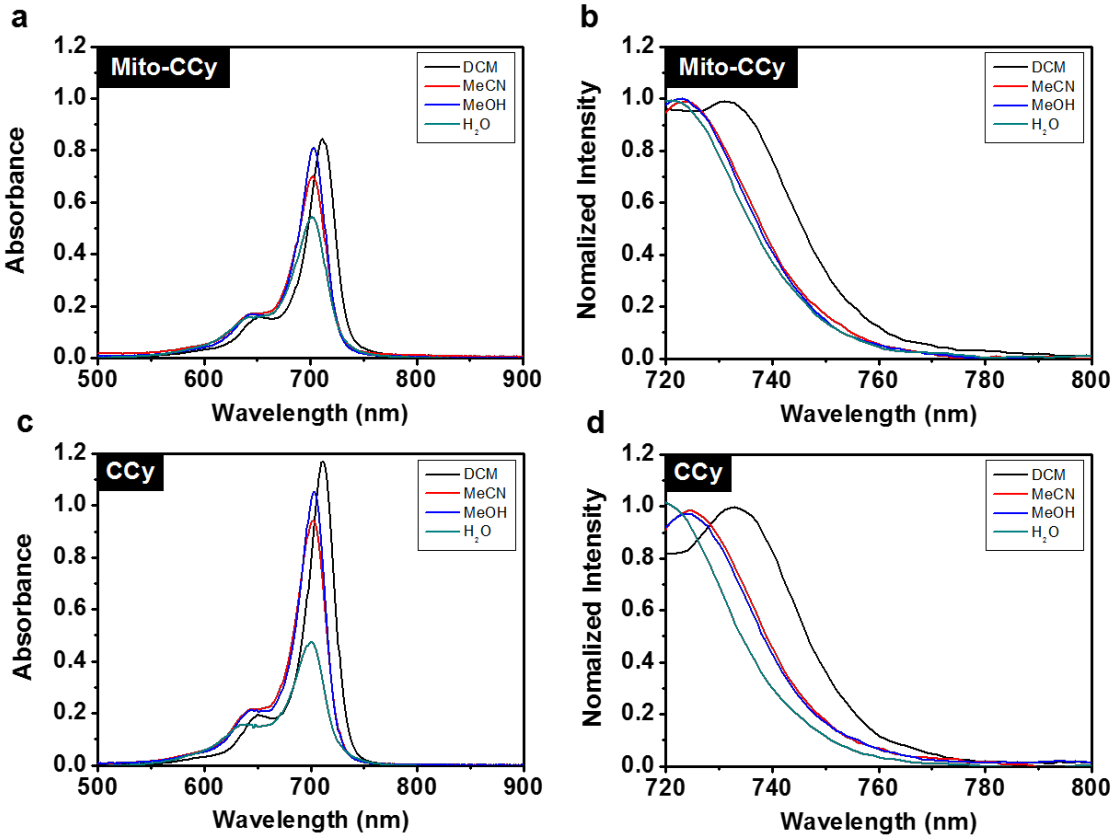

Figure S2. (a) Absorption and (b) emission spectra of **Mito-CCy** (5.0 μM) recorded in various solvents. (c) Absorption and (d) emission spectra of **CCy** (5.0 μM) recorded in various solvents. An excitation wavelength of 700 nm was used.

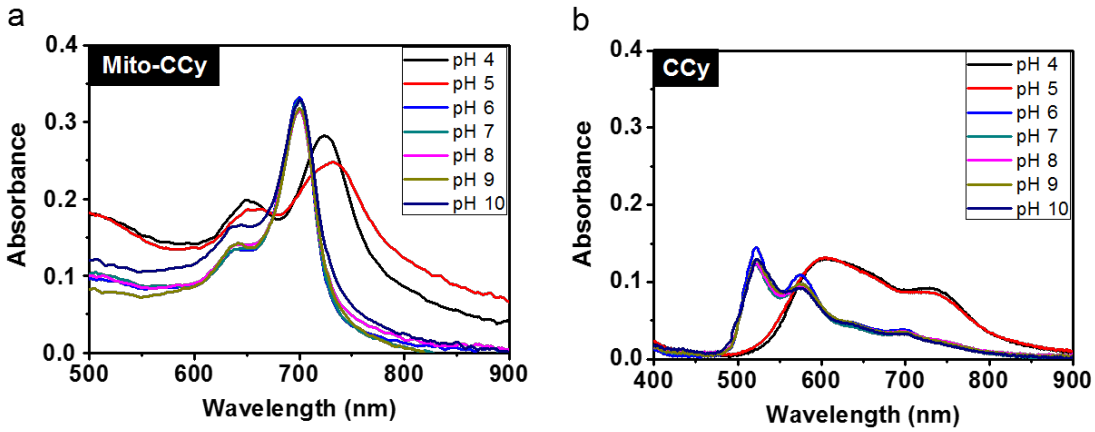

Figure S3. Absorption spectra of (a) **Mito-CCy** and (b) **CCy** recorded in 10% DMSO-buffer solution at various pH (4, 5, 6, 7, 8, 9 and 10).

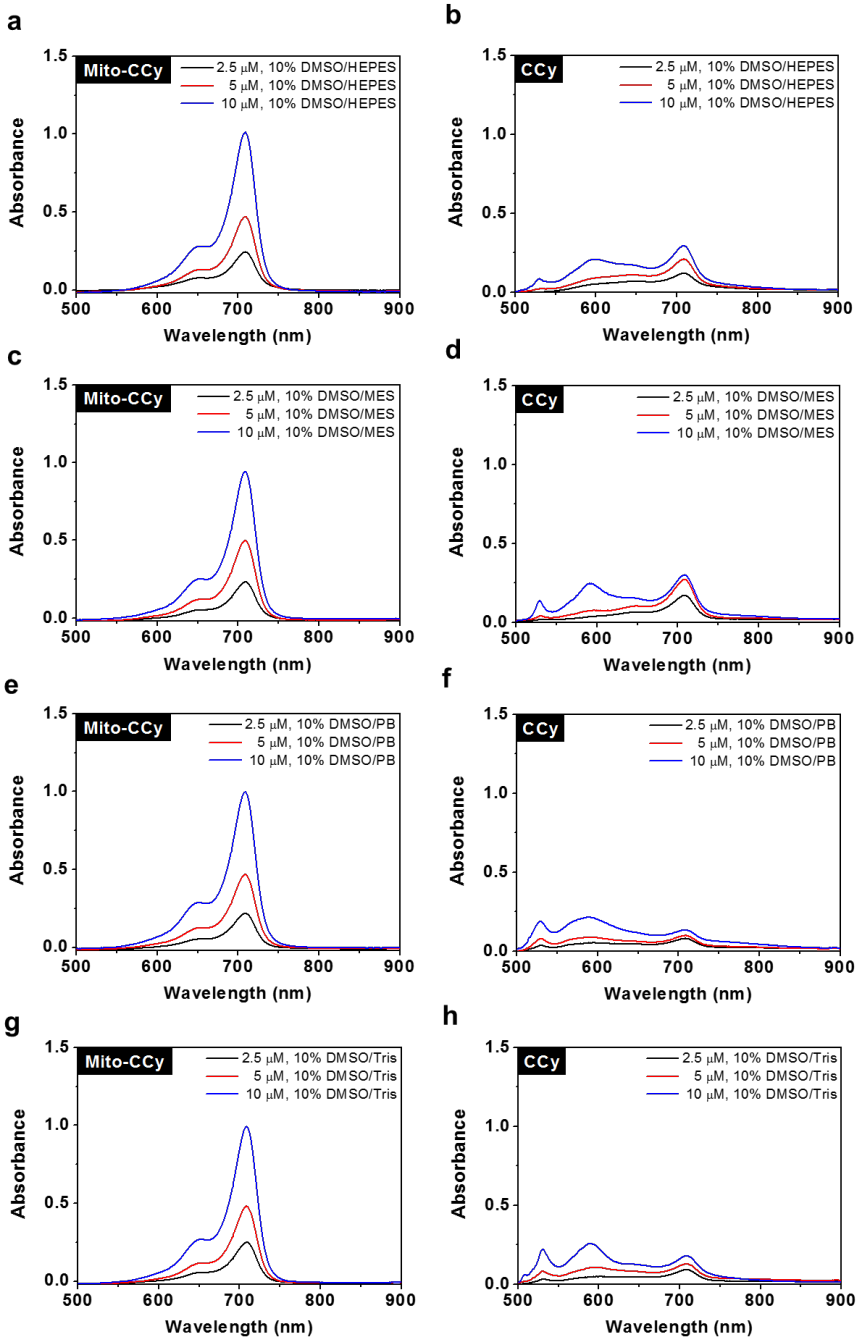

Figure S4. Absorption spectra of various concentrations (i.e., 2.5, 5.0 and 10 μM) of (a) **Mito-CCy** and (b) **CCy** in 10% DMSO-HEPES solution (pH 7.0, 10 mM HEPES), (c) **Mito-CCy** and (d) **CCy** in 10% DMSO-MES solution (pH 7.0, 10 mM MES), (e) **Mito-CCy** and (f) **CCy** in 10% DMSO-PB solution (pH 7.0, 10 mM PB) and (g) **Mito-CCy** and (h) **CCy** in 10% DMSO-Tris solution (pH 7.4, 10 mM Tris).

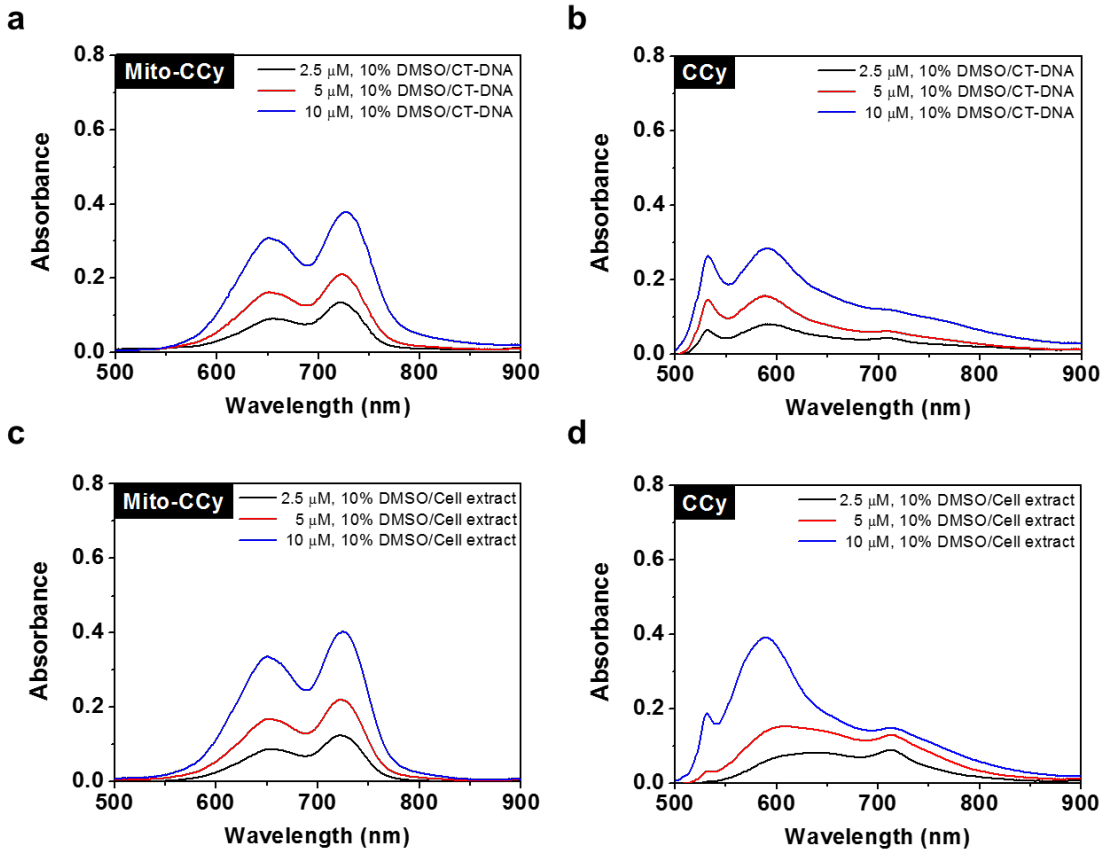

Figure S5. Absorption spectra of various concentrations (i.e., 2.5, 5.0 and 10 μM) of (a) **Mito-CCy** and (b) **CCy** in 10% DMSO-buffer solution (pH 7.4, 10 mM PBS) containing calf thymus DNA (CT-DNA: 50 μg/mL) and (c) **Mito-CCy** and (d) **CCy** in 10% DMSO-buffer solution (pH 7.4, 10 mM PBS) containing HeLa cell cytosol extract (20 μg/mL).

Table S1. Photophysical properties of indocyanine green (ICG) [a]

Compound	λ_{abs}	λ_{em}	ε (10^4 M^{-1} cm^{-1})	Φ_f	η
ICG	785	822	14.8	0.078	3.08

[a] All values measured were determined in DMSO. λ_{abs}: absorption maximum wavelength (nm). λ_{em}: emission maximum wavelength (nm). ε: molar extinction coefficient (10^4 M^{-1} cm^{-1}). Φ_f: fluorescence quantum yield. η: photothermal conversion efficiency (%).

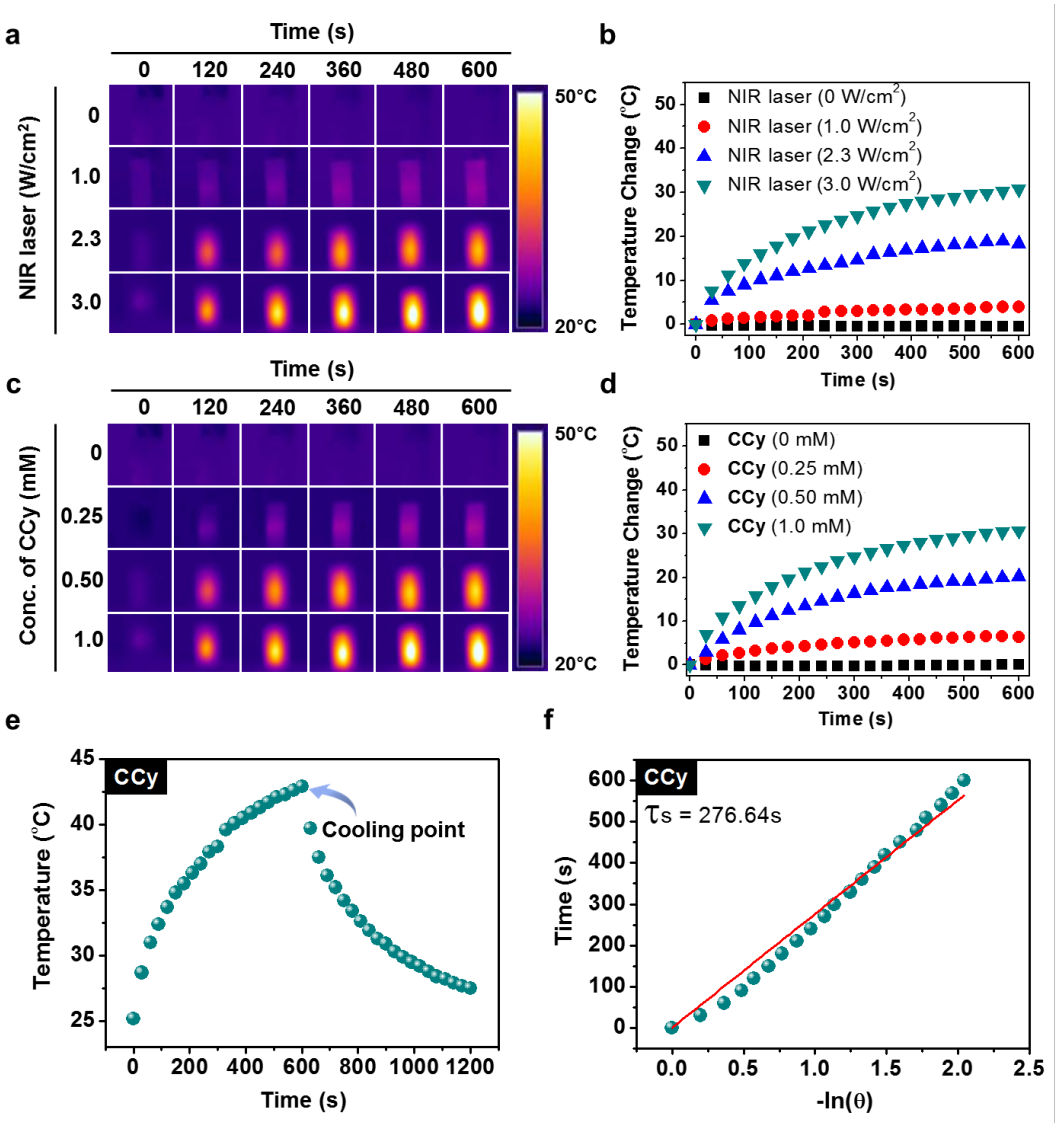

Figure S6. Photothermal conversion efficiency of **CCy.** IR thermal images of solutions containing of **CCy** at (a) 0.5 mM of **CCy** with various irradiation intensities (0, 1.0, 2.3 and 3.0 W/cm^2, 730 nm) and (c) 2.3 W/cm^2 irradiation (730 nm) with various **CCy** concentrations (0, 0.25, 0.50 and 1.0 mM) as a function of irradiation time. Photothermal heating curves of **CCy** dispersed in DMSO solution containing (b) 0.5 mM **CCy** with laser irradiation at various intensities (0, 1.0, 2.3 and 3.0 W/cm^2, 730 nm) and (d) various **CCy** concentrations (0, 0.25, 0.50 and 1.0 mM) with irradiation at 730 nm and 2.3 W/cm^2 as a function of irradiation time. (e) Photothermal effect seen upon the irradiation of **CCy** at 730 nm (laser irradiation, 2.3 W/ cm^2) for 600 s with monitoring continued after the laser was shut off. (f) Linear time data versus −ln(θ) obtained from the cooling period associated with the experiment described in (e).

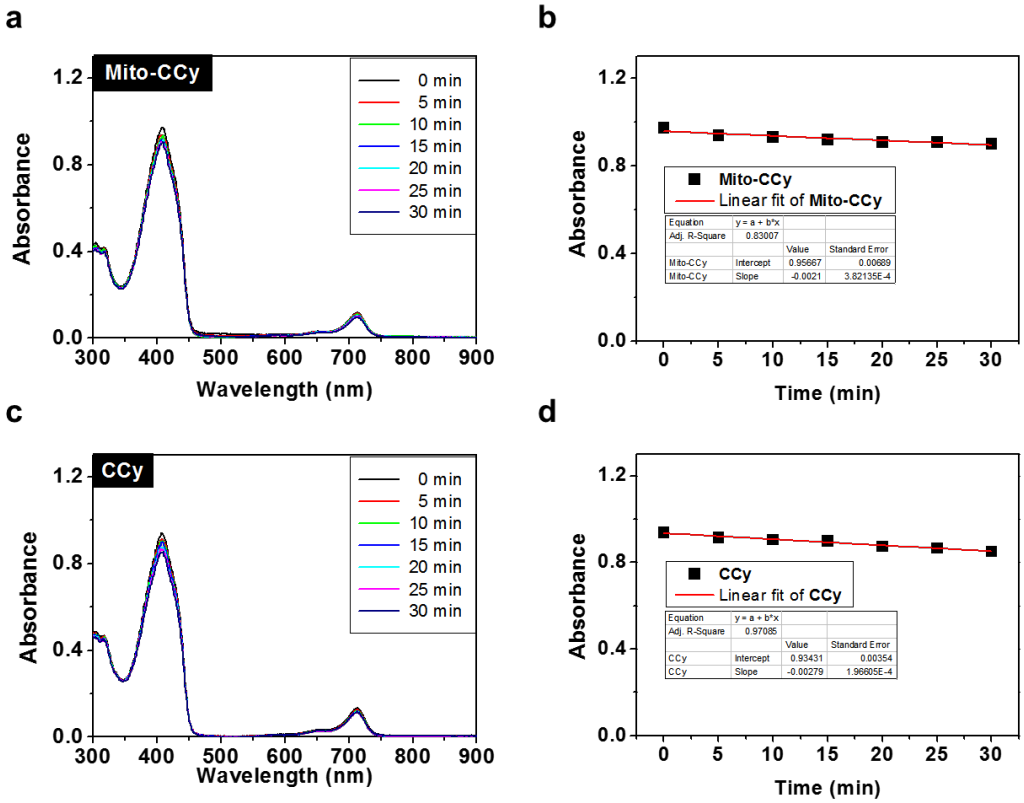

Figure S7. Change in the absorbance spectrum of the trap molecule DPBF seen in the presence of (a) **Mito-CCy** and (c) **CCy** in DMSO. (λ_{ex} = 730 nm, slit width = 15-15, Xe-lamp). Decrease in absorbance intensity of DPBF recorded at 408 nm in the presence of (b) **Mito-CCy** and (d) **CCy** in DMSO as a function of irradiation time.

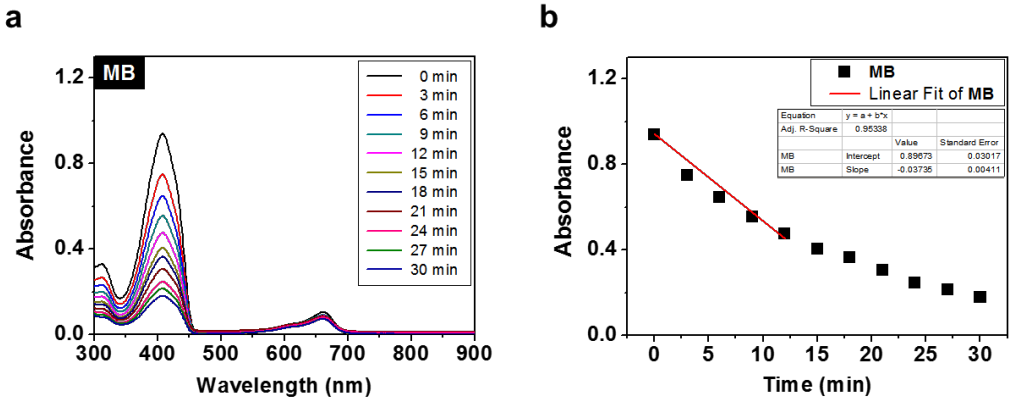

Figure S8. (a) Change in the absorbance spectrum of the trap molecule DPBF seen in the presence of Methylene Blue in DMSO. (λ_{ex} = 660 nm, slit width = 15-15, Xe-lamp). (b) Decrease in absorbance intensity of DPBF recorded at 408 nm in the presence of Methylene Blue in DMSO as a function of irradiation time.

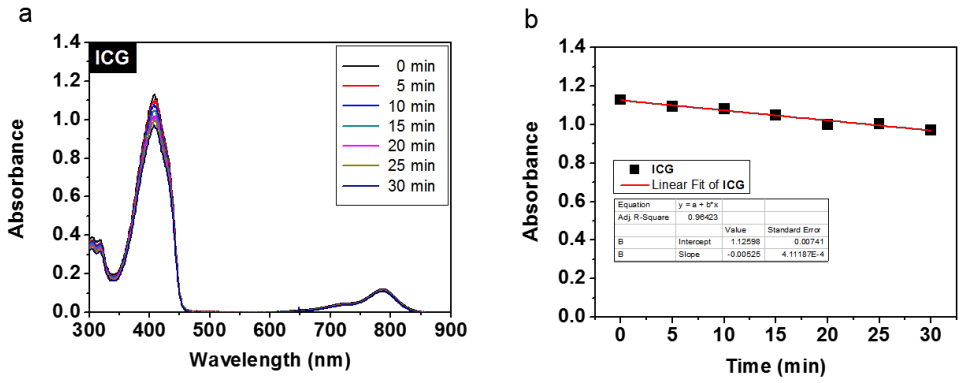

Figure S9. (a) Change in the absorbance spectrum of the trap molecule DPBF seen in the presence of ICG in DMSO. (λ_{ex} = 785 nm, slit width = 15-15, Xe-lamp). (b) Decrease in absorbance intensity of DPBF recorded at 408 nm in the presence of ICG in DMSO as a function of irradiation time.

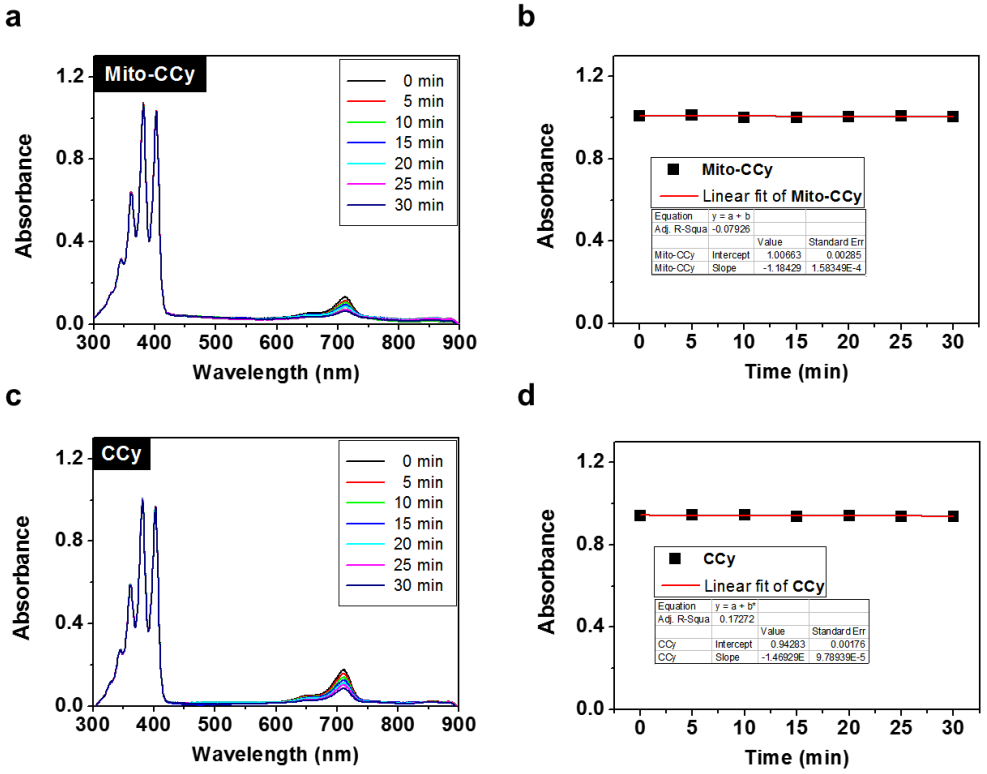

Figure S10. Change in the absorbance spectrum of an aqueous soluble trap molecule, 9,10-anthracenediyl-bis(methylene)dimalonic acid (ABDA), seen in the presence of (a) **Mito-CCy** and (c) **CCy** in 20% DMSO-buffer solution (pH 7.4, 10 mM PBS) (λ_{ex} = 730 nm, slit widths = 15-15, Xe-lamp). Decrease in the absorbance intensity of ABDA recorded at 382 nm in the presence of (b) **Mito-CCy** and (d) **CCy** in 20% DMSO-buffer solution (pH 7.4, 10 mM PBS) as a function of irradiation time.

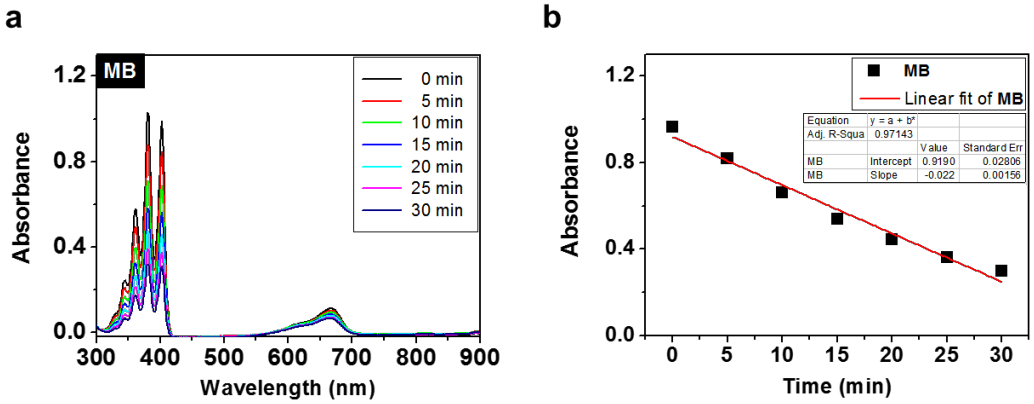

Figure S11. (a) Change in the absorbance spectrum of an aqueous soluble trap molecule 9,10-anthracenediyl-bis(methylene)dimalonic acid (ABDA) seen in the presence of MB in 20% DMSO-buffer solution (pH 7.4, 10 mM PBS) (λ_{ex} = 660 nm, slit width = 15-15, Xe-lamp). (b) Decrease in absorbance intensity of ABDA recorded at 382 nm in the presence of MB in 20% DMSO-buffer solution (pH 7.4, 10 mM PBS) as a function of irradiation time.

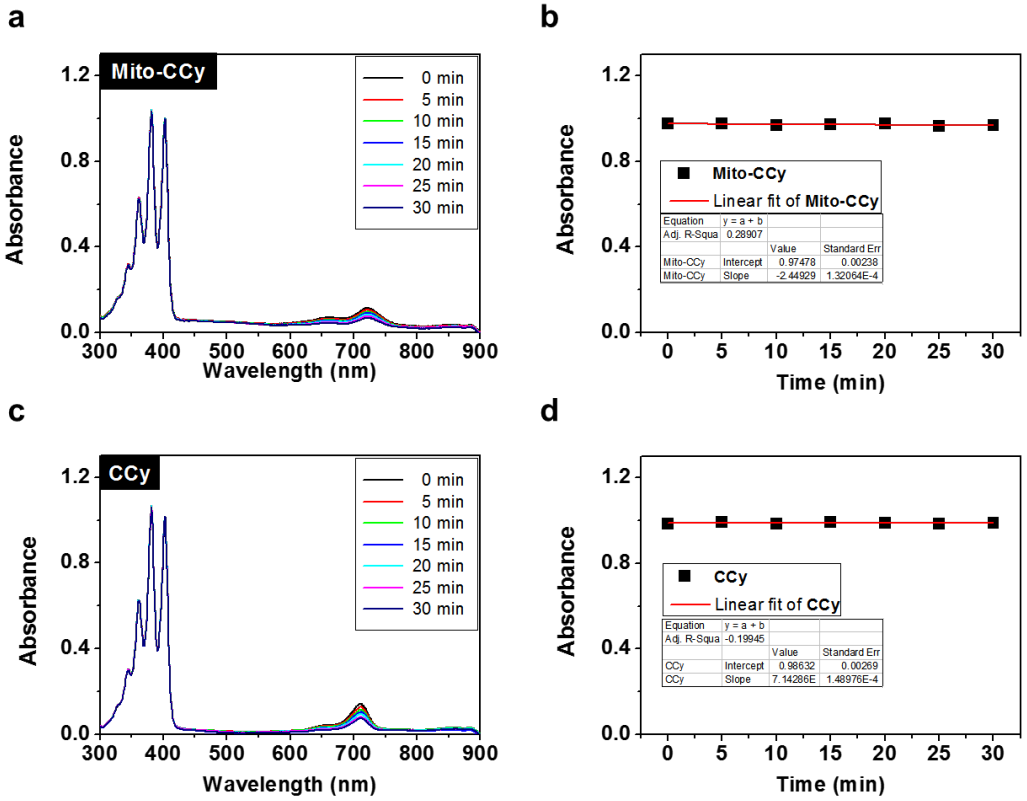

Figure S12. Change in the absorbance spectrum of an aqueous soluble trap molecule 9,10-anthracenediyl-bis(methylene)dimalonic acid (ABDA) seen in the presence of (a) **Mito-CCy** and (c) **CCy** in 20% DMSO-buffer solution (pH 7.4, 10 mM PBS) including calf thymus DNA (CT-DNA: 50 μg/mL) (λ_{ex} = 730 nm, slit width = 15-15, Xe-lamp). Decrease in the absorbance intensity of ABDA recorded at 382 nm in the presence of (b) **Mito-CCy** and (d) **CCy** in a 20% DMSO-buffer solution mixture (pH 7.4, 10 mM PBS) that included calf thymus DNA (CT-DNA: 50 μg/mL) as a function of irradiation time.

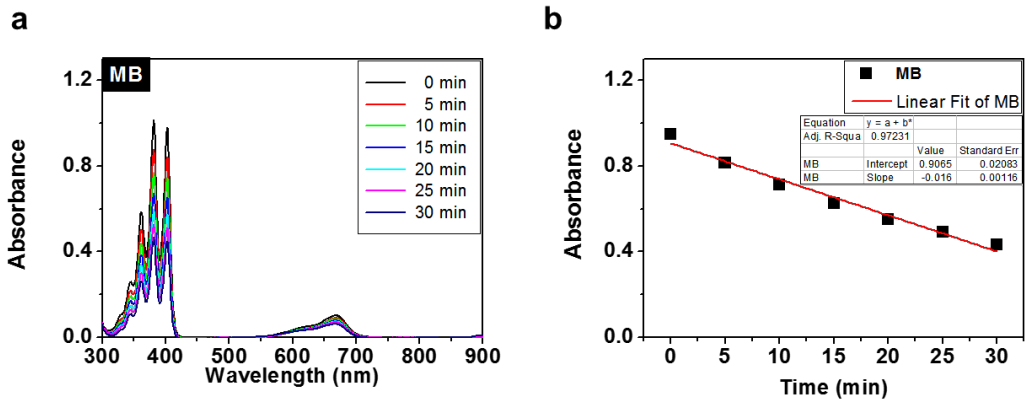

Figure S13. (a) Change in the absorbance spectrum of the aqueous soluble trap molecule 9,10-anthracenediyl-bis(methylene)dimalonic acid (ABDA) seen in the presence of MB in 20% DMSO-buffer solution (pH 7.4, 10 mM PBS) containing calf thymus DNA (CT-DNA: 50 μg/mL) (λ_{ex} = 660 nm, slit width = 15-15, Xe-lamp). (b) Decrease in absorbance intensity of ABDA recorded at 382 nm in the presence of MB in 20% DMSO-buffer solution (pH 7.4, 10 mM PBS) containing calf thymus DNA (CT-DNA: 50 μg/mL) as a function of irradiation time.

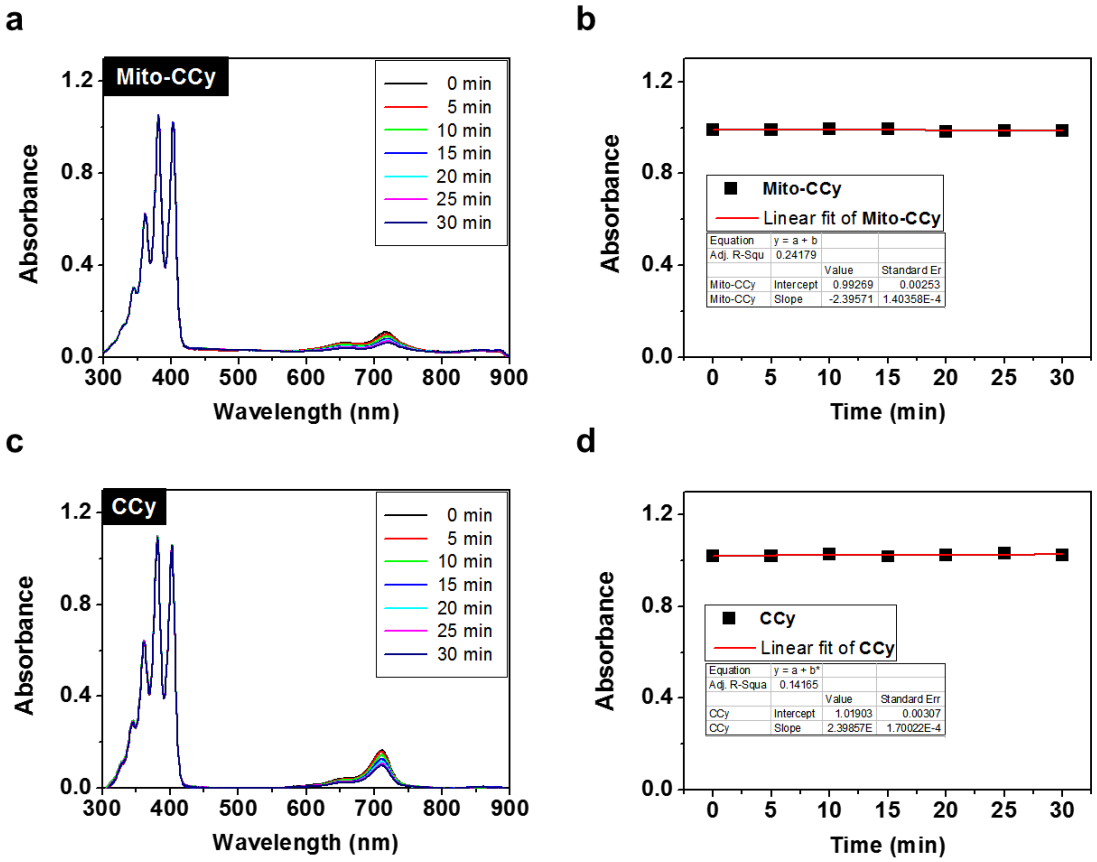

Figure S14. Change in the absorbance spectrum of the aqueous soluble trap molecule 9,10-anthracenediyl-bis(methylene)dimalonic acid (ABDA) seen in the presence of (a) **Mito-CCy** and (c) **CCy** in 20% DMSO-buffer solution (pH 7.4, 10 mM PBS) that includes HeLa cell cytosol extract (20 μg/mL) (λ_{ex} = 730 nm, slit widths = 15-15, Xe-lamp). Decrease in absorbance intensity of ABDA recorded at 382 nm in the presence of (b) **Mito-CCy** and (d) **CCy** in 20% DMSO-buffer solution (pH 7.4, 10 mM PBS) containing HeLa cell cytosol extract (20 μg/mL) as a function of irradiation time.

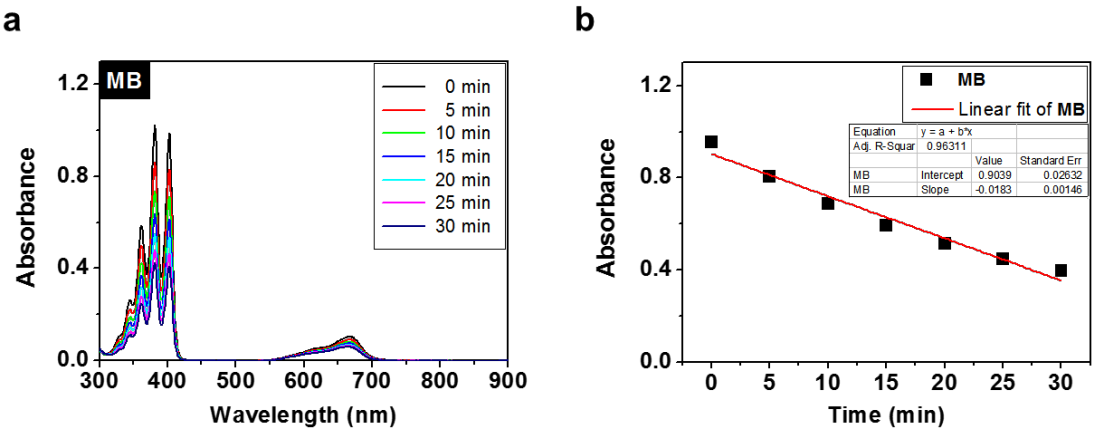

Figure S15. (a) Change in the absorbance spectrum of the aqueous soluble trap molecule 9,10-anthracenediyl-bis(methylene)dimalonic acid (ABDA) seen in the presence of MB in 20% DMSO-buffer solution (pH 7.4, 10 mM PBS) containing HeLa cell cytosol extract (20 μg/mL) (λ_{ex} = 660 nm, slit widths = 15-15, Xe-lamp). (b) Decrease in absorbance intensity of ABDA recorded at 382 nm in the presence of MB in 20% DMSO-buffer solution (pH 7.4, 10 mM PBS) containing HeLa cell cytosol extract (20 μg/mL) as a function of irradiation time.

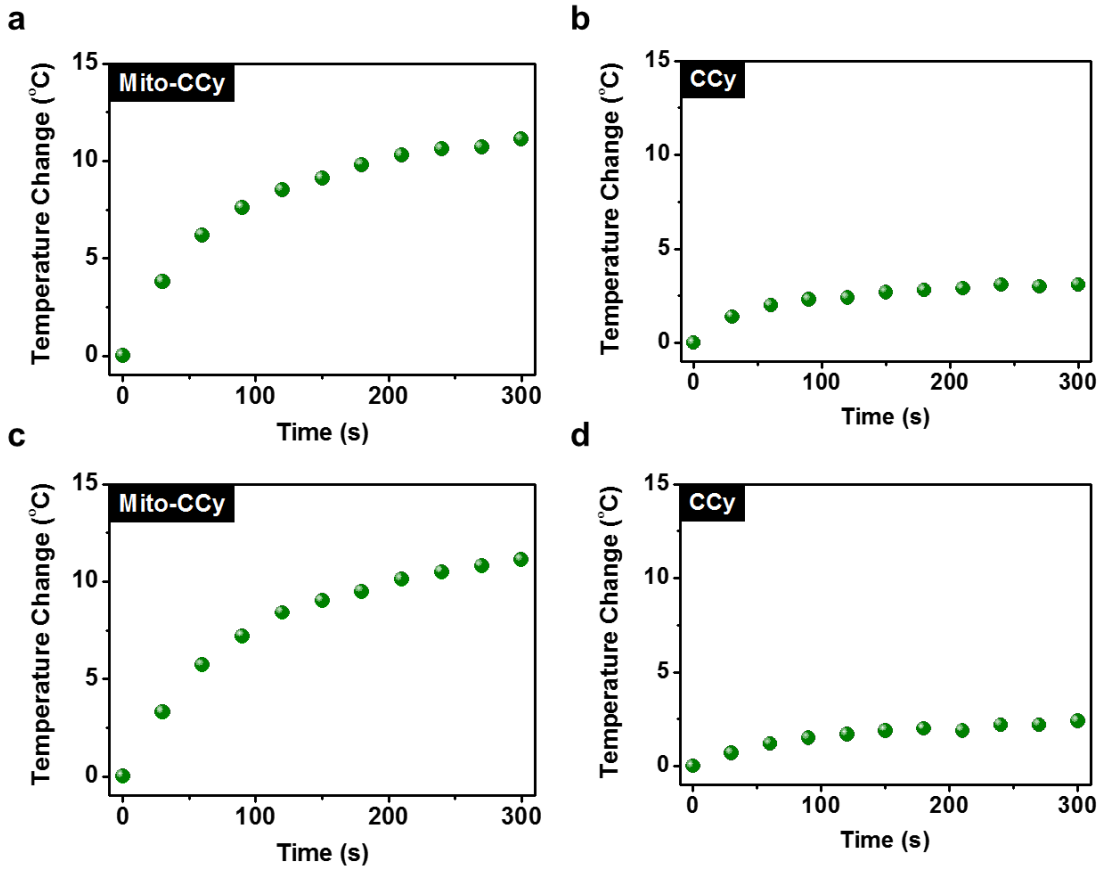

Figure S16. Photothermal heating curves of **Mito-CCy** and **CCy**. **Mito-CCy** (a) and **CCy** (b) (0.5 mM, respectively) dispersed in 50% DMSO-buffer solution (pH 7.4, 10 mM PBS) containing calf thymus DNA (CT-DNA: 50 μg/mL) with 730 nm laser irradiation (2.3 W/cm^2) as a function of irradiation time. **Mito-CCy** (c) and **CCy** (d) (0.5 mM, respectively) dispersed in 50% DMSO-buffer solution (pH 7.4, 10 mM PBS) containing HeLa cell cytosol extract (20 μg/mL) with 730 nm laser irradiation (2.3 W/cm^2) as a function of irradiation time.

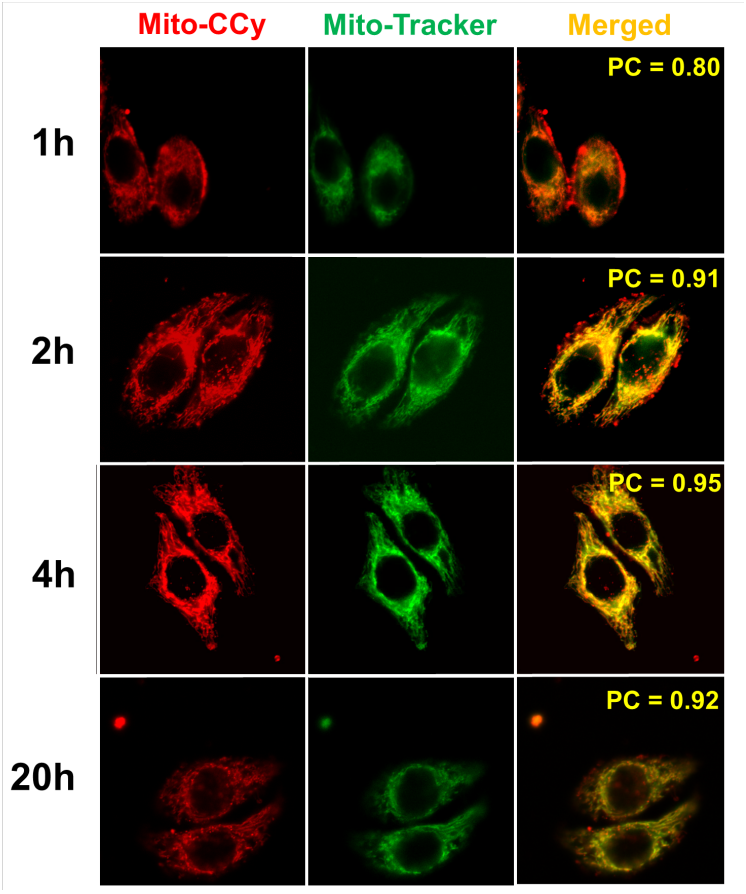

Figure S17. Confocal microscopic images of **Mito-CCy** co-localized with MitoTracker Green FM in HeLa cells. HeLa cells were incubated with **Mito-CCy** (2.0 μM) for 1, 2, 4, and 20 h and then treated with MitoTracker Green FM (0.05 μM) for 15 min. Separate and merged images of the fluorescence of **Mito-CCy** and MitoTracker Green FM. The fluorescence images were collected using 488 nm and 633 nm light for excitation and detection, respectively, with 505−530 nm band pass (green) and 650 nm long pass (red) filters being employed as warranted.

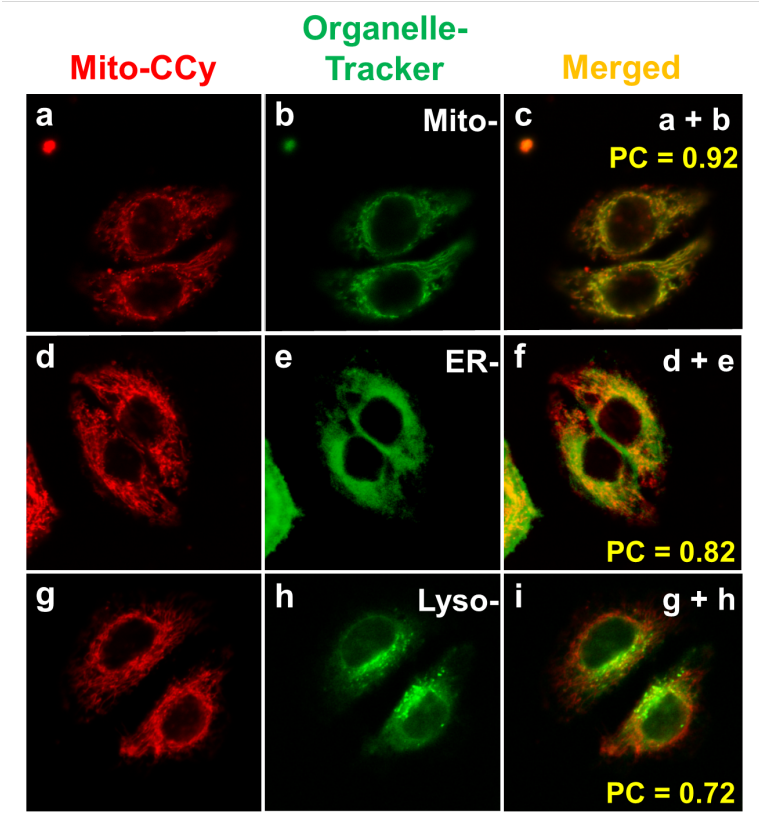

Figure S18. Confocal microscopic images of **Mito-CCy** co-localized with various commercially available organelle trackers in HeLa cells. (a, d, and g). HeLa cells were incubated with **Mito-CCy** (2.0 μM) for 20 h and then with (b) MitoTracker Green FM (0.05 μM), (e) ER Tracker Green (1.0 μM), or (h) Lysotracker Green DND-26 (0.05 μM) for 15 min. (c) Merged image of (a) and (b). (f) Merged image of (d) and (e). (i) Merged image of (g) and (h). The fluorescence images of the organelle trackers and **Mito-CCy** were collected using 488 nm and 633 nm light for excitation and detection, respectively, with 505−530 nm band pass (green) and 650 nm long pass (red) filters being employed as warranted.

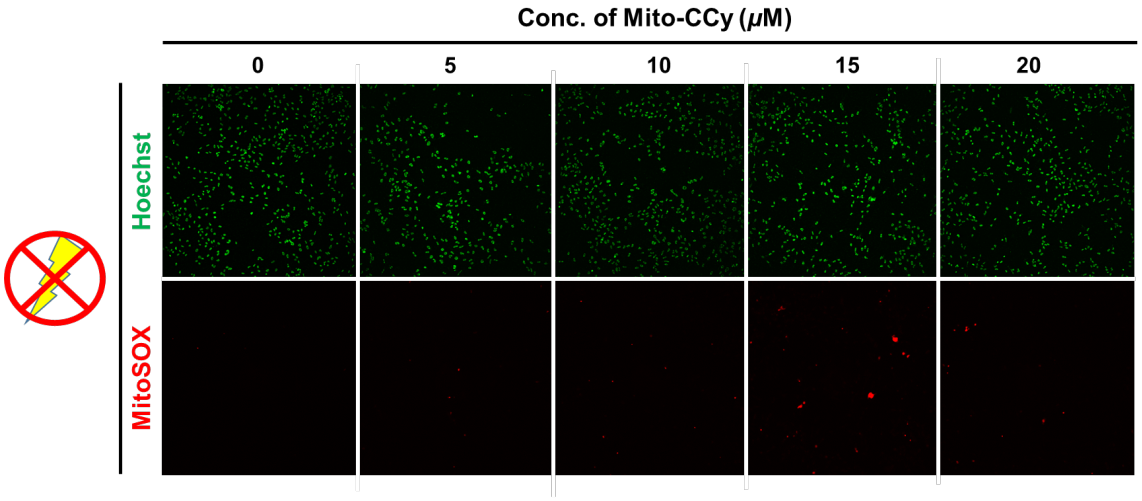

Figure S19. Cytotoxicity observed for HeLa cells incubated with **Mito-CCy**. Confocal fluorescence images of HeLa cells obtained after incubation with **Mito-CCy** as a function of concentration for 4 h. Dead cells are labeled in red by staining with PI, whereas all cells were visualized using Hoechst 33342 (green).

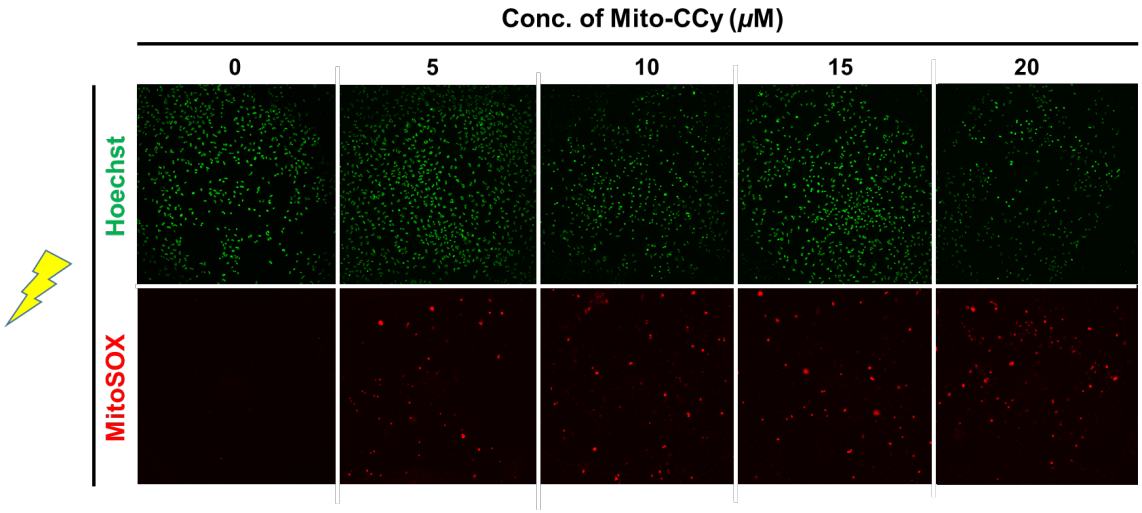

Figure S20. Cytotoxicity observed for HeLa cells incubated with **Mito-CCy**. Confocal fluorescence images of HeLa cells obtained after incubation with **Mito-CCy** for 4 h following 730 nm laser irradiation (2.3 W/cm^2) for 10 min as a function of concentrations. Live/dead cells are observed as green or red by staining with Hoechst 33342 and PI, respectively.

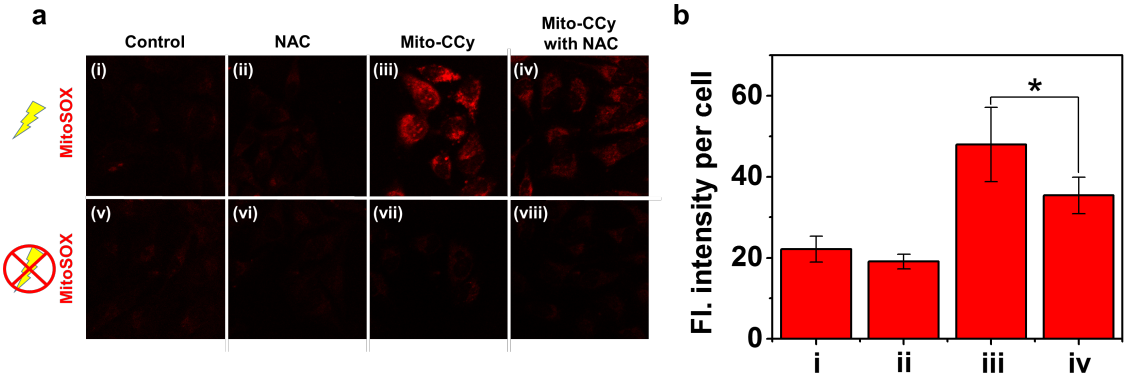

Figure S21. Confocal fluorescence microscopic images of HeLa cells treated with MitoSOX (1 μM) (i) without and with co-incubation with (ii) NAC (5 mM), (iii) **Mito-CCy** (10 μM), and (iv) **Mito-CCy** (10 μM) and NAC (5 mM) upon subjecting to 730 nm NIR irradiation (2.3 W/cm^2) for 10 min (top set of photos). Confocal fluorescence microscopic images of HeLa cells treated with MitoSOX (1 μM) (v) without and with co-incubation with (vi) NAC (5 mM), (vii) **Mito-CCy** (10 μM), and (viii) **Mito-CCy** (10 μM) and NAC (5 mM) in the absence of 730 nm NIR irradiation (lower). (b) Fluorescence intensity per cell. *P < 0.05. Fluorescence was collected using an excitation wavelength of 488 nm and recording the emission at 550−650 nm (red).

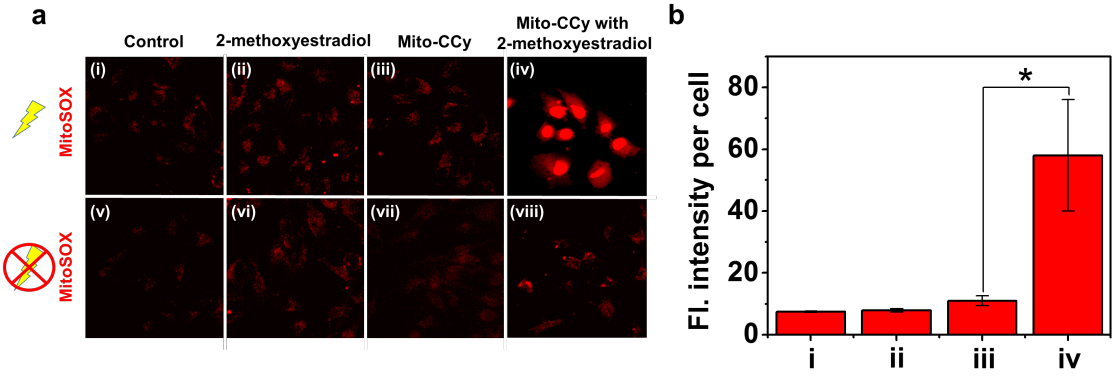

Figure S22. Confocal fluorescence microscopic images of HeLa cells treated with MitoSOX (1 μM) (i) without and with co-incubation in the presence of (ii) 2-methoxyestradiol (2 μM), (iii) **Mito-CCy** (10 μM) and (iv) **Mito-CCy** (10 μM) with 2-methoxyestradiol (2 μM) with NIR irradiation (730 nm; 2.3 W/cm^2) for 10 min (upper trace). Confocal fluorescence microscopic images of HeLa cells treated with MitoSOX (1 μM) (v) without and with co-incubation in the presence of (vi) 2-methoxyestradiol (2 μM), (vii) **Mito-CCy** (10 μM) and (viii) **Mito-CCy** (10 μM) with 2-methoxyestradiol (2 μM) in the absence of 730 nm NIR irradiation (lower). (b) Fluorescence intensity per cell. *P < 0.05. Fluorescence was collected using an excitation wavelength of 488 nm and recording the emission at 550−650 nm (red).

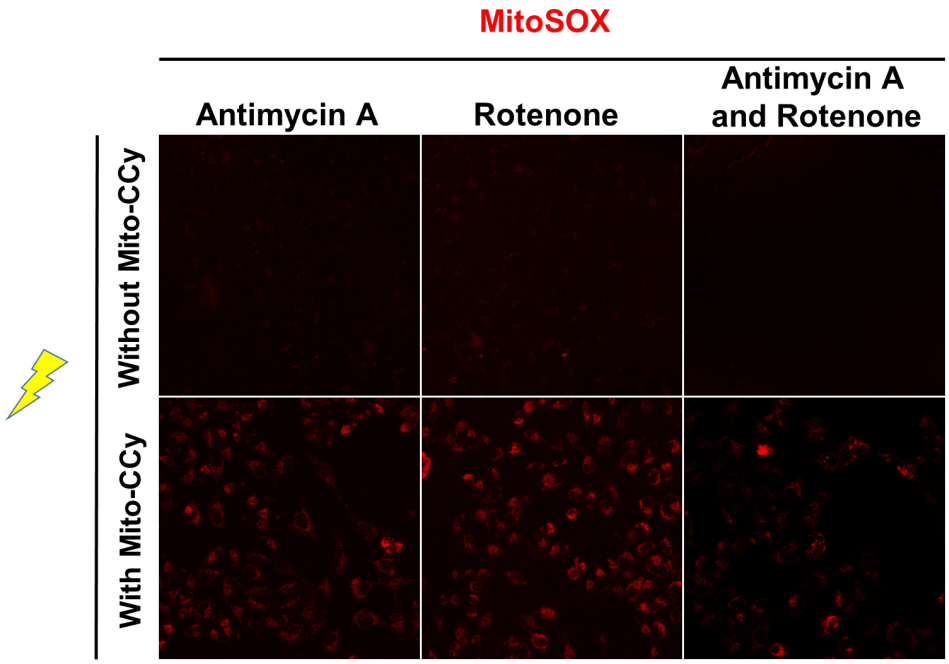

Figure S23. Confocal fluorescence microscopic images of HeLa cells treated with MitoSOX (1 μM) with 730 nm NIR irradiation (2.3 W/cm^2) for 10 min without (upper) and with **Mito-CCy** (10 μM) (lower). Microscopic images that serve to compare from left to right the effect of antimycin A (0.5 μM), rotenone (0.5 μM), and antimycin A (0.5 μM) with rotenone (0.5 μM). Fluorescence was collected using an excitation wavelength of 488 nm and recording the emission at 550−650 nm (red).

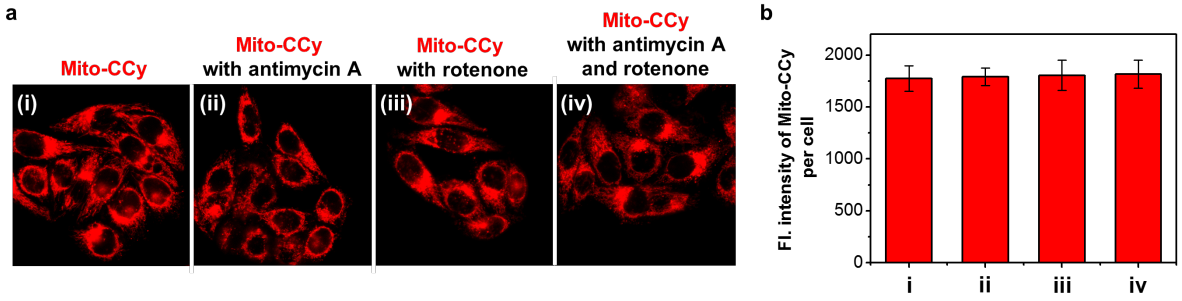

Figure S24. (a) Confocal fluorescence microscopic images of HeLa cells treated with **Mito-CCy** (10 μM) for 4 h (i) without and with co-incubation with (ii) antimycin A (0.5 μM), (iii) rotenone (0.5 μM), and (iv) antimycin A (0.5 μM) with rotenone (0.5 μM). (b) Fluorescence intensity per cell. Fluorescence images were recorded using 633 nm excitation and 650 nm long pass emission (red) wavelengths, respectively.

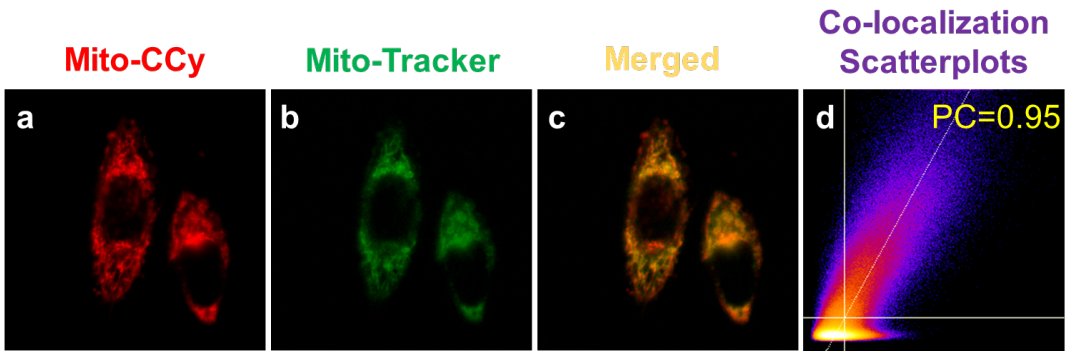

Figure S25. Confocal microscopic images of **Mito-CCy** co-localized with Mito tracker green in HeLa cells. (a) HeLa cells were incubated with **Mito-CCy** (2.0 μM) for 4 h and then with (b) MitoTracker Green FM (0.05 μM) for 30 min followed by antimycin A (0.5 μM) and rotenone (0.5 μM) for 30 min. The cells were washed 3 times with DMEM. (c) Merged image of (a) and (b). (d) Co-localization scatterplots of (c). PC:0.95. The fluorescence images of the organelle trackers and **Mito-CCy** were collected using 488 nm and 633 nm light for excitation and detection, respectively, with 505−530 nm band pass (green) and 650 nm long pass (red) filters being employed as warranted.

- **^{1}H NMR and ^{13}C NMR spectra**

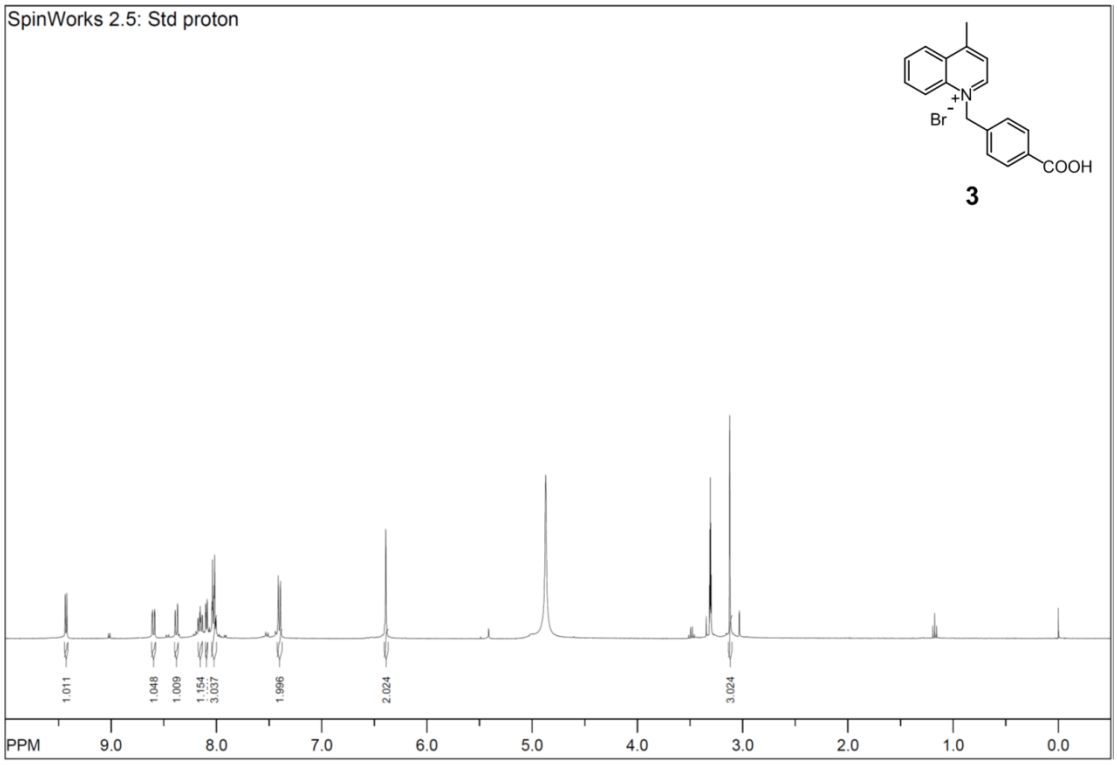

Figure S26. ^{1}H NMR spectrum (400 MHz) of **3** recorded in MeOH-d_4.

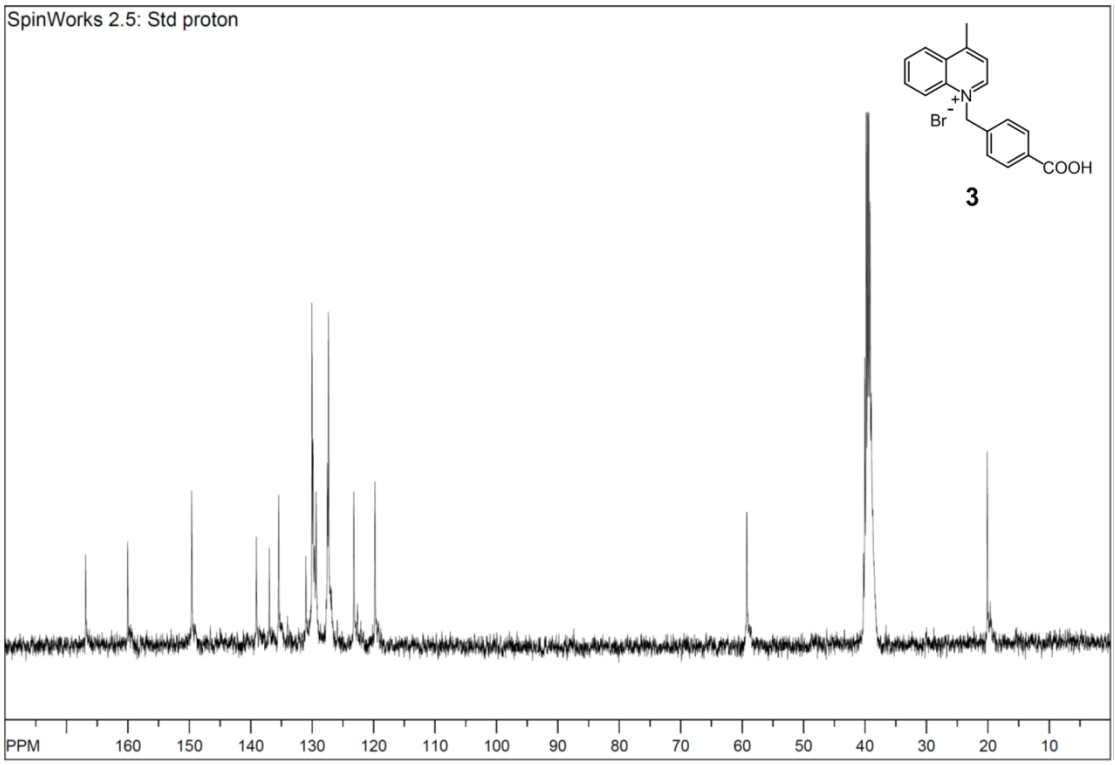

Figure S27. ^{13}C NMR spectrum (100 MHz) of **3** recorded in DMSO-d_6.

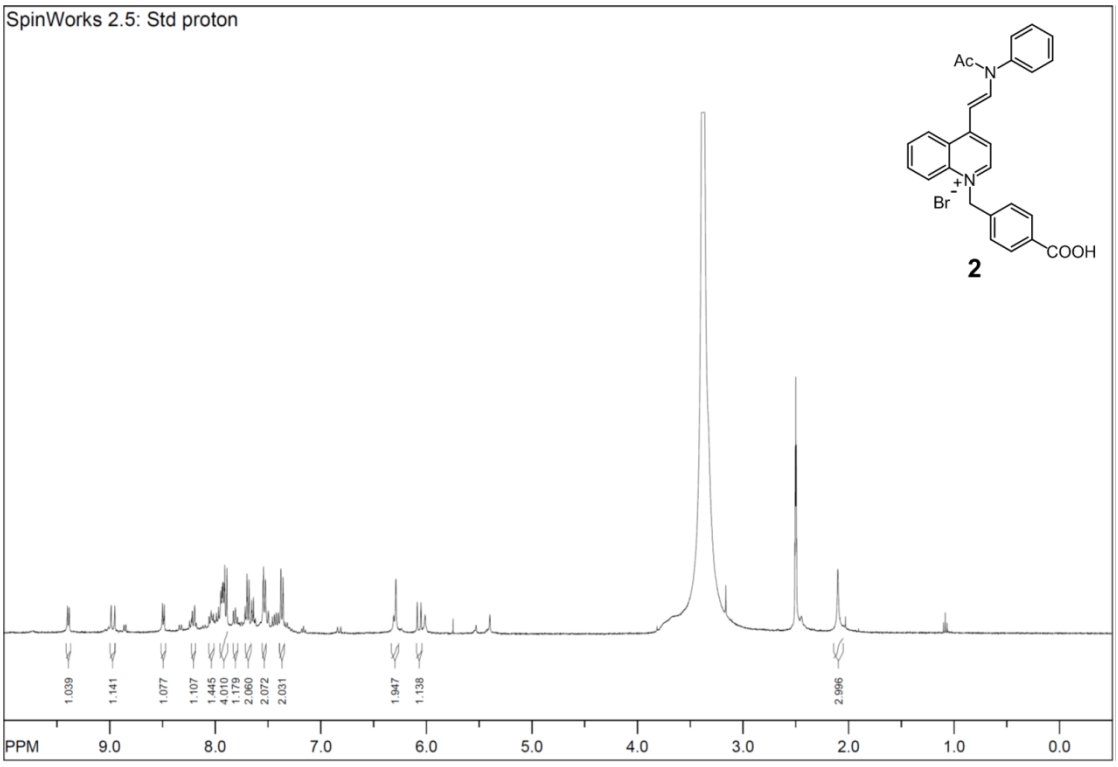

Figure S28. ^{1}H NMR spectrum (400 MHz) of **2** recorded in DMSO-d_6.

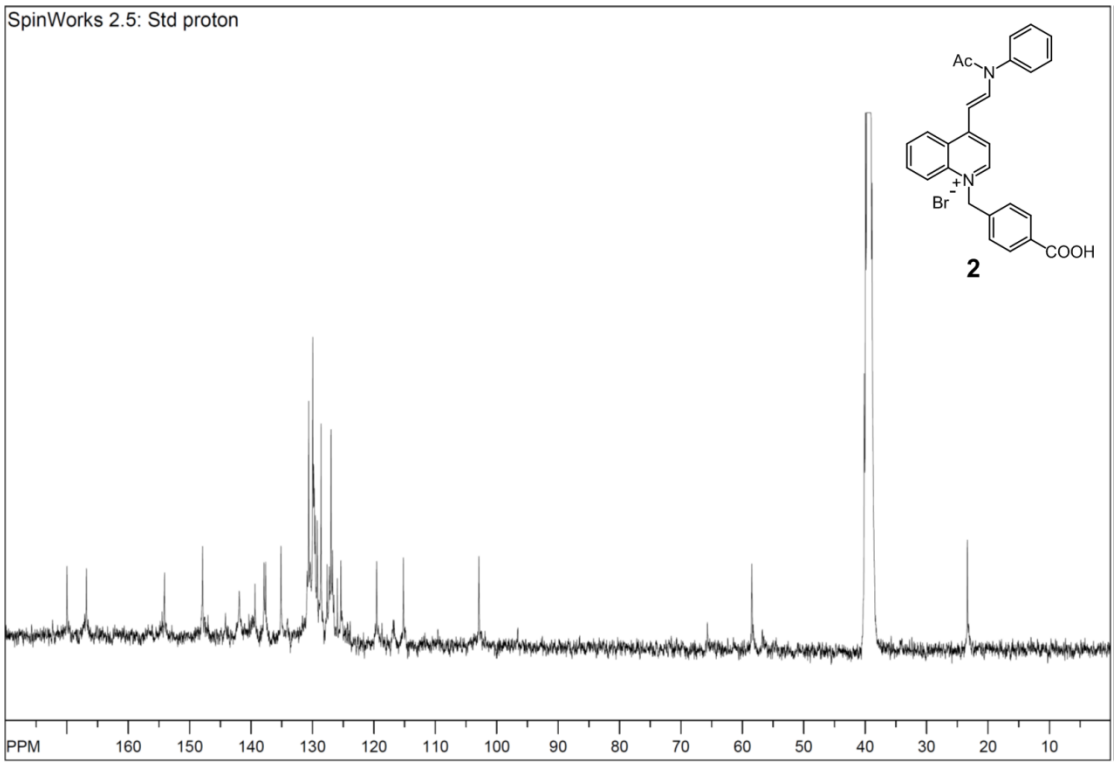

Figure S29. ^{13}C NMR spectrum (100 MHz) of **2** recorded in DMSO-d_6.

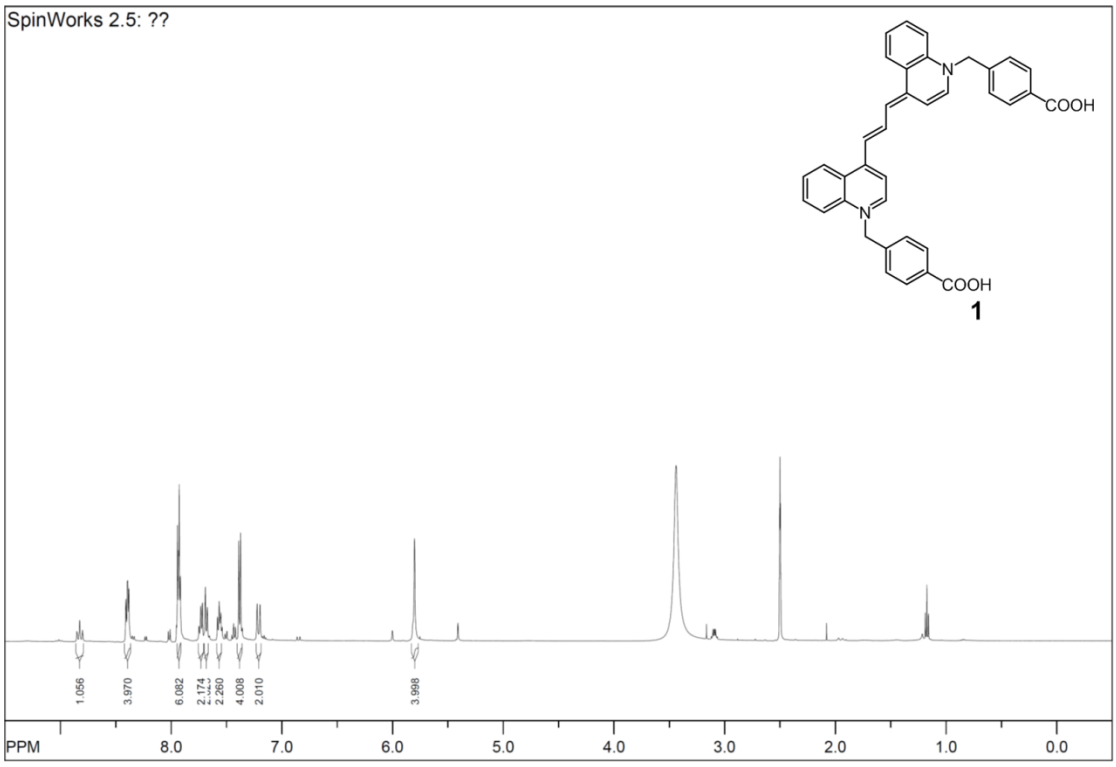

Figure S30. ^{1}H NMR spectrum (500 MHz) of **1** recorded in DMSO-d_6.

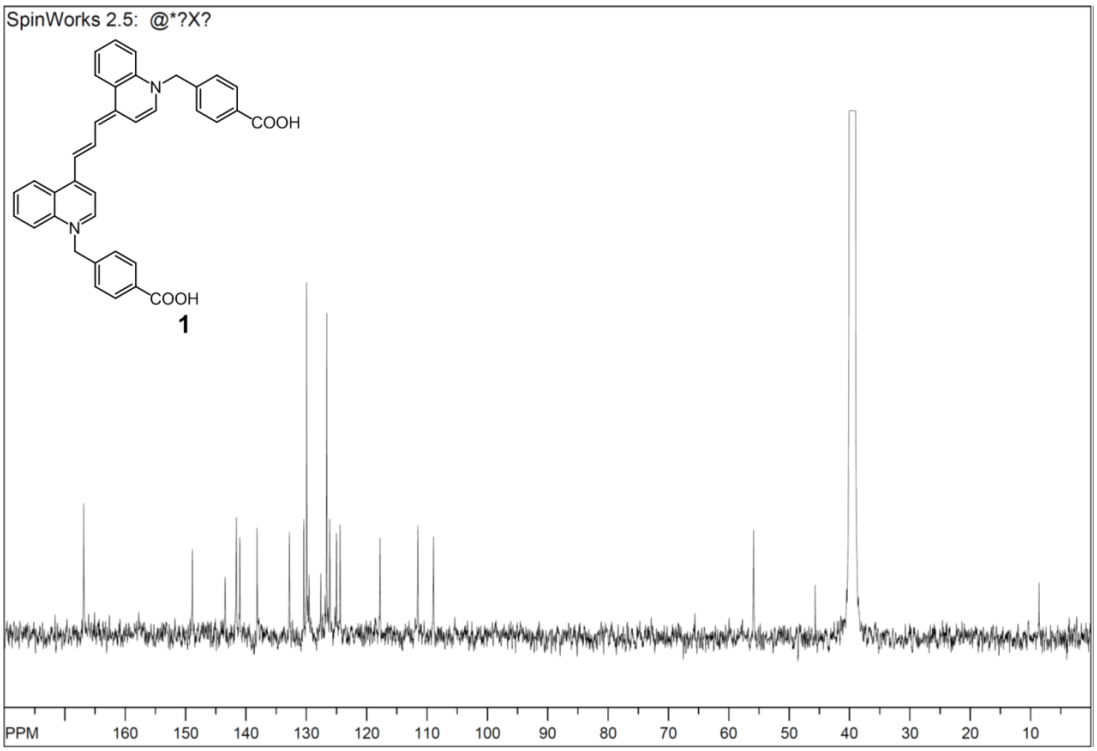

Figure S31. ^{13}C NMR spectrum (125 MHz) of **1** recorded in DMSO-d_6.

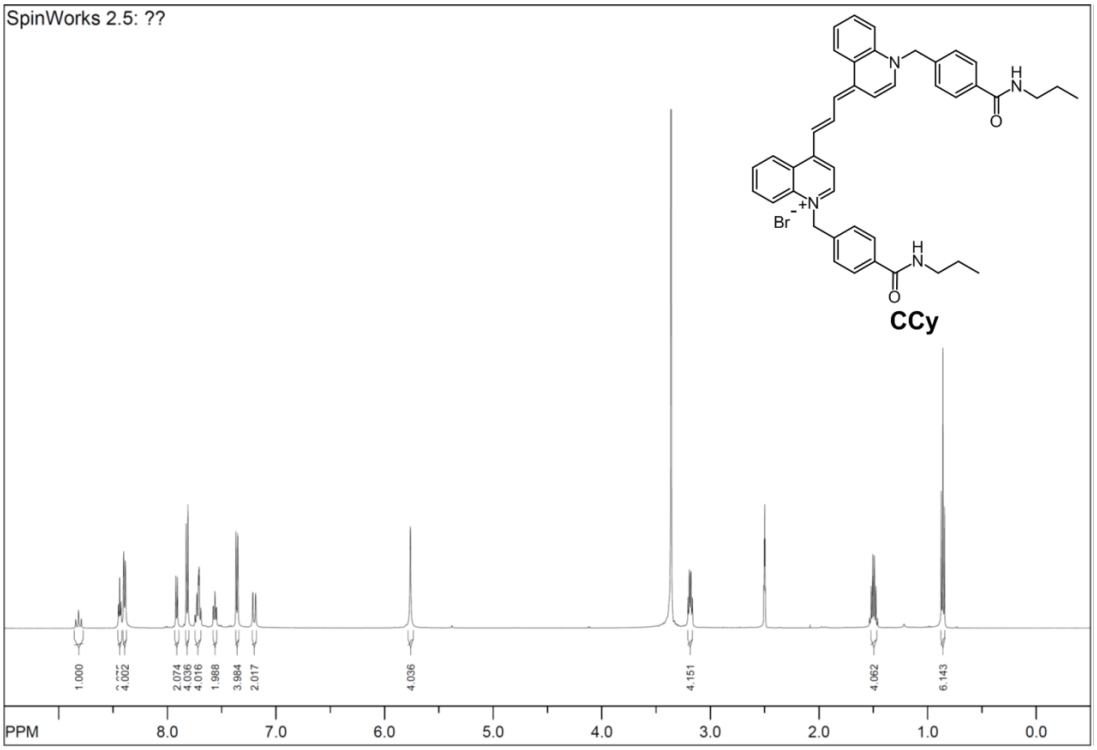

Figure S32. ^{1}H NMR spectrum (500 MHz) of **CCy** recorded in DMSO-d_6.

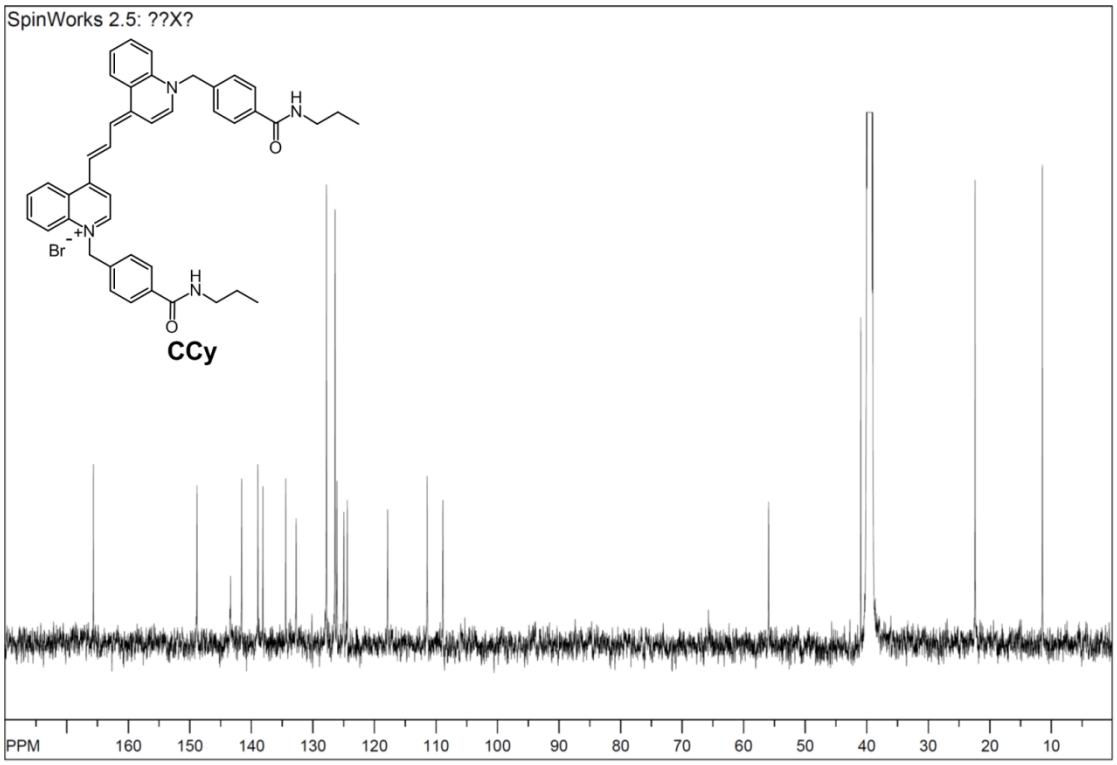

Figure S33. ^{13}C NMR spectrum (125 MHz) of **CCy** recorded in DMSO-d_6.

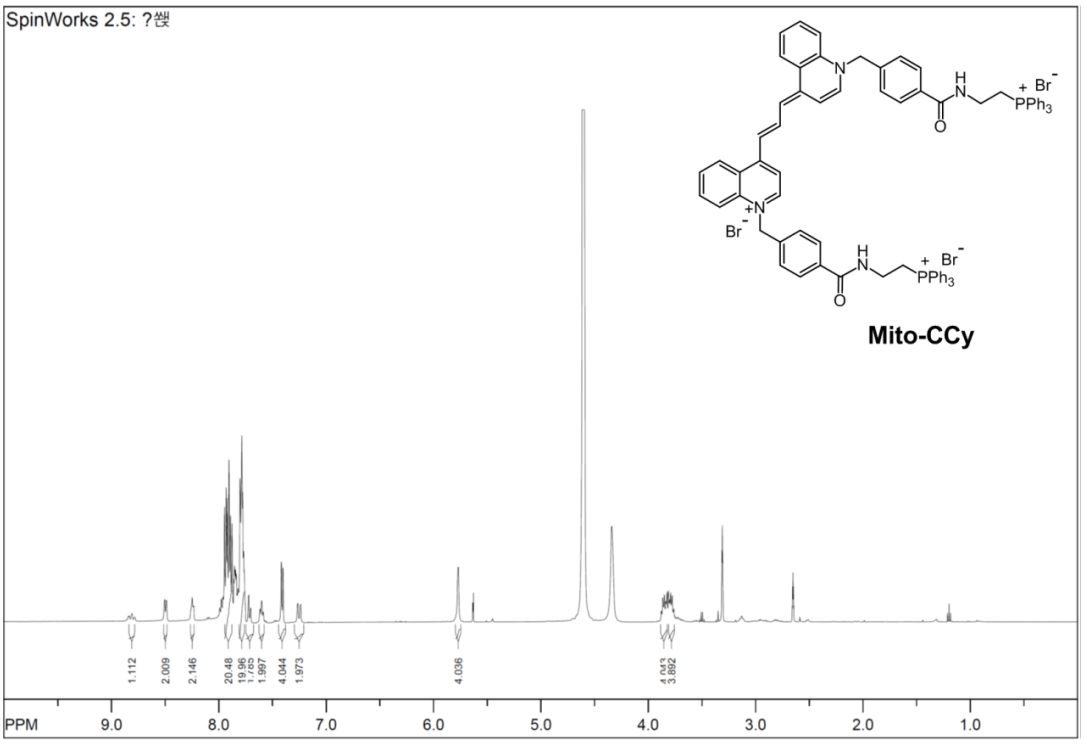

Figure S34. [1]H NMR spectrum (500 MHz) of **Mito-CCy** recorded in MeOH-d_4/DMSO-d_6.

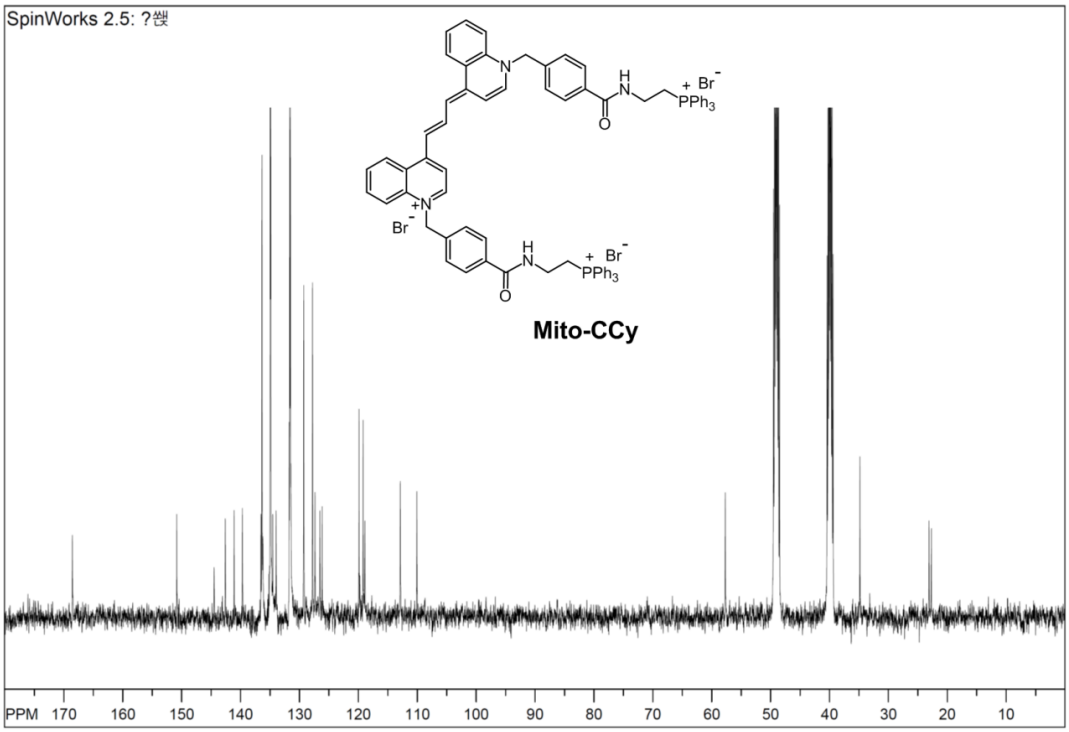

Figure S35. [13]C NMR spectrum (125 MHz) of **Mito-CCy** in MeOH-d_4/DMSO-d_6.

- **ESI-MS spectra**

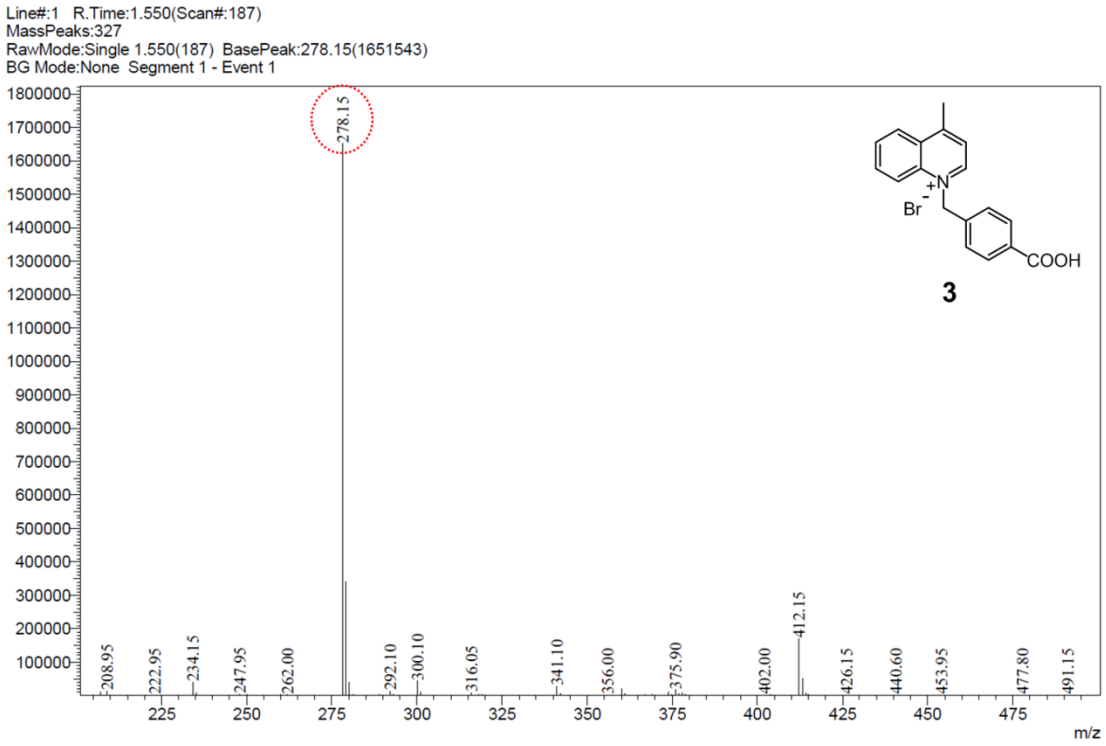

Figure S36. ESI-MS spectrum of **3**.

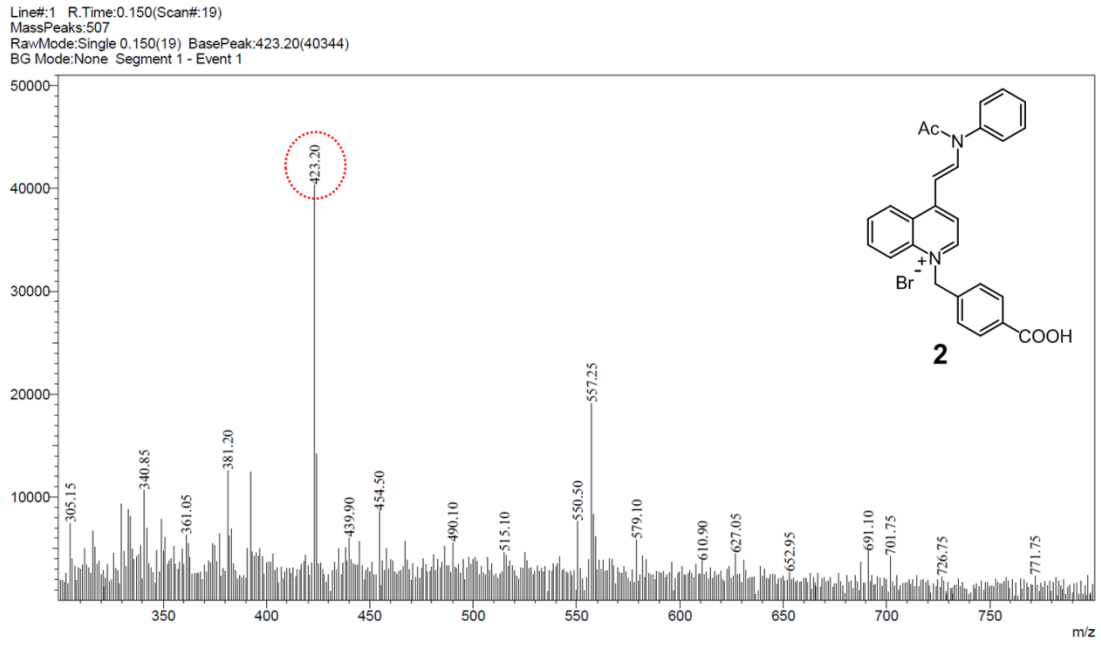

Figure S37. ESI-MS spectrum of **2**.

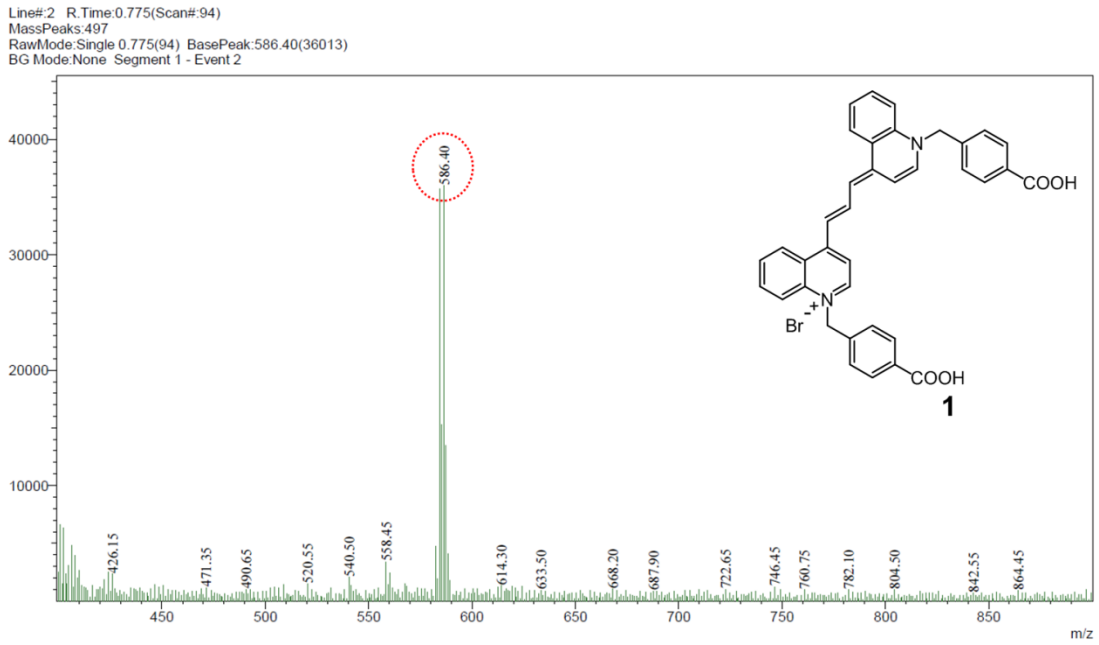

Figure S38. ESI-MS spectrum of **1**.

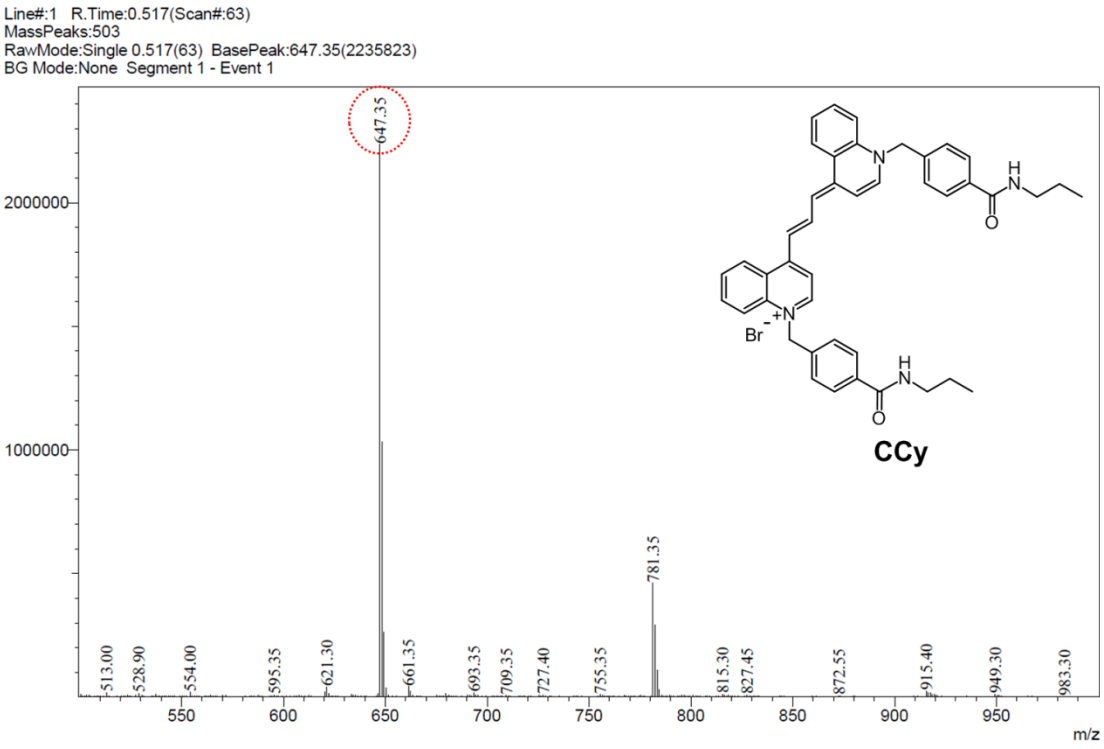

Figure S39. ESI-MS spectrum of **CCy**.

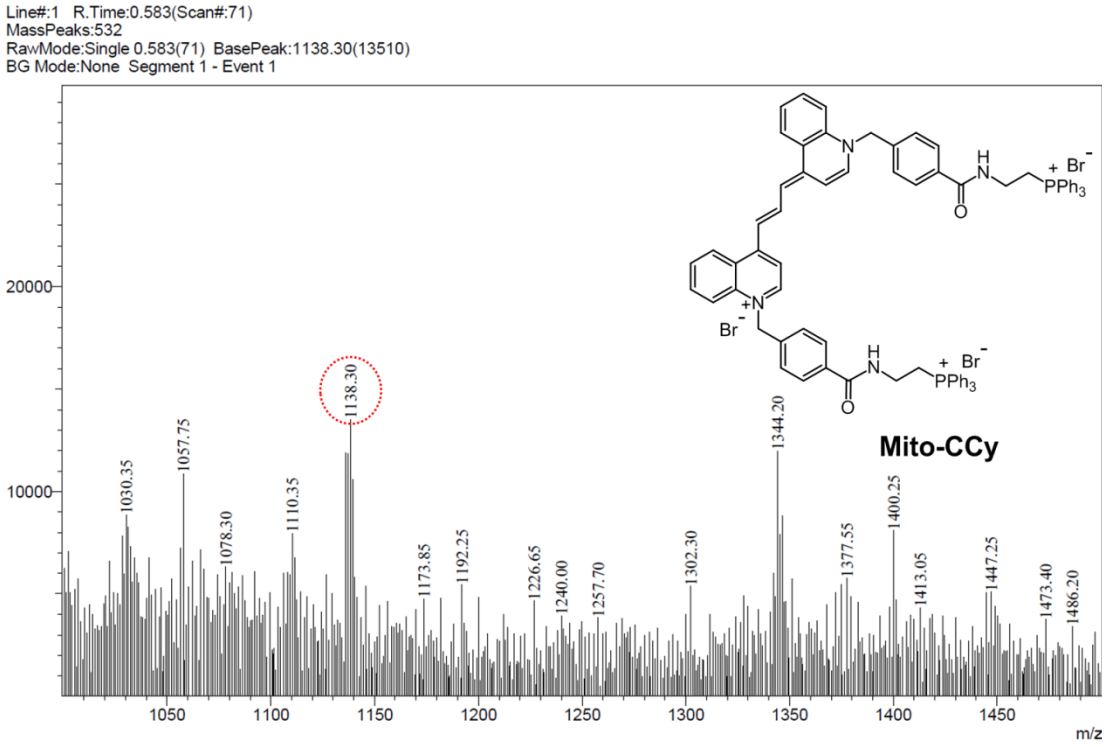

Figure S40. ESI-MS spectrum of **Mito-CCy**.

References

1. Maryanoff, B. E.; Reitz, A. B.; Duhl-Emswiler, B. A. *J. Am. Chem. Soc.* **1985**, *107*, 217–226.
2. Vincett, P. S.; Voigt, E. M.; Rieckhoff, K. E. *J. Phys. Chem.* **1971**, *55*, 4131–4140.
3. Tian, Q. W.; Jiang, F. R.; Zou, R. J.; Liu, Q.; Chen, Z. G.; Zhu, M. F.; Yang, S. P.; Wang, J. L.; Wang, J. H.; Hu, J. Q. *ACS Nano* **2011**, *5*, 9761–9771.
4. Adarsh, N.; Avirah, R. R.; Ramaiah, D. *Org. Lett*. **2010**, *12*, 5720–5723.
5. Mirenda, M.; Strassert, C. A.; Dicelio, L. E.; San Roman, E. *ACS, Appl. Mater. Interfaces* **2010**, *2*, 1556–1560.